

A mathematical framework to study organising principles in graphical representations of biochemical processes

Aditya Chaudhuri¹, Ralf Köhl^{2,3}, and Olaf Wolkenhauer^{4,5,6}

¹University of Rostock, Institute of Computer Science, Rostock, Germany.

²Christian-Albrechts-University Mathematics Seminar, Kiel, Germany.

³Kiel Nano, Surface and Interface Science, Christian-Albrechts-University, Kiel, Germany

⁴University of Rostock, Department of Systems Biology & Bioinformatics, Rostock, Germany.

⁵Leibniz-Institute for Food Systems Biology; Technical University of Munich, Freising; Germany

⁶Stellenbosch Institute for Advanced Study, South Africa

Systems Biology Graphical Notation (SBGN) is a standardised notational system that visualises biochemical processes as networks. These visualizations lack a formal framework, so that the analysis of such networks through modelling and simulation is an entirely separate task, determined by a chosen modelling framework (e.g. differential equations, Petri nets, stochastic processes, graphs). A second research gap is the lack of a mathematical framework to compose network representations. The complexity of molecular and cellular processes forces experimental studies to focus on subsystems. To study the functioning of biological systems across levels of structural and functional organisation, we require tools to compose and organise networks with different levels of detail and abstraction.

We address these challenges by introducing a category-theoretic formalism for biochemical processes visualised using SBGN Process Description (SBGN-PD) language. Using the theory of structured cospans, we construct a symmetric monoidal double category and demonstrate its horizontal 1-morphisms as SBGN Process Descriptions. We obtain organisational principles such as *compositionality* (building a large SBGN-PD from smaller ones) and *zooming-out* (abstracting away details in biochemical processes) defined in category-theoretic terms. We also formally investigate how a particular portion of a biochemical network influences the remaining portion of the network and vice versa. Throughout the paper, we illustrate our findings using standard SBGN-PD examples.

1 Introduction

Information about biological processes is available in databases, for which KEGG [22] is a widely known example. Various markup languages, like KEGG ML [24] or BioPax [15], have been developed to represent biological processes graphically. Encoding of biological processes as networks allows linking a graphical representation with molecular information, including references to the literature, links to gene and disease ontologies, and links to databases containing further chemical and structural information. For quantitative analyses of biological processes, we need to translate the network representation to a mathematical model. To this end, markup languages like CellML [4], PharmML [40], and SBML [16, 21, 23] allow the encoding of mathematical models in a stan-

Aditya Chaudhuri: aditya.chaudhuri@uni-rostock.de, chaudhuriaditya@gmail.com,  0000-0002-1703-5889

Ralf Köhl: koehl@math.uni-kiel.de,  0000-0003-0105-0029

Olaf Wolkenhauer: olaf.wolkenhauer@uni-rostock.de,  0000-0001-6105-2937

standardized computational format. The BioModels database [29] is a repository providing over 1000 models of biological processes encoded in SBML.

Systems Biology Graphical Notation (SBGN) [25] has been developed to promote an efficient, unambiguous exchange and reuse of biological information related to signalling pathways, metabolic networks, and gene regulatory networks within the scientific community. Over the years, SBGN has become a widely used standardised graphical notational system to visualise biological processes at different level of detail. For SBGN, there is also a markup language called SBGNML [11], which allows efficient exchange of SBGN encoded biological data to other commonly used systems biology markup languages like BioPAX or SBML, and between tools supporting SBGN (eg. CellDesigner [17, 18], Newt [10, 37], Krayon [43], SBGN-ED [14], STON [42], cd2sbgnml [2], and MINERVA [19]).

SBGN offers three different but complimentary visual languages, namely *Process Description* (SBGN-PD) [35], *Activity Flow* (SBGN-AF) [31] and *Entity Relationship* (SBGN-ER) [39], each focussing on a different level of abstraction. SBGN-PD works at the detailed biochemical reaction level, SBGN-AF represents the connections and interactions between biochemical entities in terms of information flow, and SBGN-ER shows how entities influence each other's actions and behaviours. However, SBGN is only a visual tool and is not a mathematical representation of biological processes. There have been a few attempts to fill the gap between the SBGN visualisations and mathematical representations, including [34], which formalised SBGN-PD diagrams using asynchronous automata networks, or [28] using Hybrid Functional Petri Net (HFPN) and [13] using textual representations (SBGNtext). However, all these attempts do not support the study of *organising principles*, specifically,

- (a) formal ways to compose a collection of biochemical molecular/cellular networks into a composite network and decompose a large network into smaller subcomponents,
- (b) formal ways to zoom in and zoom out details in a biochemical molecular/cellular network,
- (c) formal compatibility features between the said compositionality and the said process of zooming-out and zooming-in details,
- (d) formal ways to study how a particular portion of a network depends on the entities produced outside it, and conversely, how the network outside this particular portion depends on the entities produced inside the said portion.

To this day, most experimental studies will only be able to address subsystems, parts of a larger whole. There is, thus, a need to compose networks, and ideally, we must have tools available to study the organisation of large networks independent of the simulation framework chosen. Taking human diseases as an example, virtually all processes linked to a disease phenotype involve various cell types and many molecule types. The Atlas of Inflammation Resolution (AIR) [38] is an example where information for over twenty thousand reactions involved in the resolution of acute inflammation is gathered. Processes of this size are never studied as a whole. Experimental studies are usually focusing on, and are practically limited to, networks of relatively small sizes. Thus, especially when the target network size is very large, formal organisational principles, as stated above, and a formal framework of graphical representations, which abstracts from concrete modelling and simulation formalisms, are expected to be helpful for quantitative and qualitative analyses.

Our present manuscript uses Applied Category Theory (ACT), especially Baez et al.'s theory of structured cospans in the framework of symmetric monoidal double categories [6] to develop the previously mentioned organising principles for biochemical molecular and cellular networks admitting SBGN-PD visualisations. The framework of symmetric monoidal double categories has been previously successfully used to study the composition of networks, where horizontal 1-morphisms represent subsystems with interfaces. Examples close to our goal are reaction networks modeled with Petri nets [1, 7, 9]. For example, in [1], Aduddell et al. introduced a compositional framework for Petri nets with signed links to model regulatory biochemical networks. These works and the availability of large numbers of SBGN-encoded networks motivated our present effort. Since SBGN also allows features like compartments and submaps, we hope our formal compositional framework would provide us with a new perspective to study multilevelness in biological systems. With the

increasing availability of SBGN-PD visualisations in biological databases, formal organisational principles for a generic SBGN-PD would provide biologists with generic methods to analyse the behaviour of a generic biochemical reaction network at multi scales, irrespective of the network size.

Before we move on to the paper’s organisation, we say a few words about our choice to use Applied Category Theory for our goal. For the last decade or so, ACT has established itself as a Category Theory-based discipline in mathematics for studying the behaviour of large-scale systems by composing the behaviour of its subsystems. It has been successfully applied to a wide range of areas, including biochemical regulatory networks [1], chemical reaction networks [8, 9], Markov processes [33], epidemiological modelling [5, 26], data structures [3, 12, 32], game theory [20], deterministic dynamical system [27] etc., to name a few. In fact, ACT-based frameworks allow a level of abstraction or generalisation that encompasses a range of concrete modelling approaches like Petri Nets [7–9], ODEs [7, 8], stochastic processes [33], graphs [1, 30], to name a few, and their *functorial interrelationships* (interrelationships which respect compositionality in a suitable way). Many of the ACT-based formalisations have also been successfully translated into user-friendly software for the purpose of computational studies via platforms like Algebraic Julia [41]. The framework presented in this paper contributes to these efforts, by focusing on graphical visualizations of biochemical processes.

1.1 Structure of the Paper

The paper is organised as follows. In Section 2, we illustrate our main results informally through some standard examples of biochemical reaction networks visualised in SBGN Process Description. We begin formally developing our theory in Section 3. Subsection 3.1 introduces the notion of *process networks* and *process species*, which model biochemical reaction networks and biochemical reactions, respectively, and illustrate these notions through some standard SBGN Process Descriptions. In Subsection 3.2, we introduce the notion of a *morphism of process networks* and derive some of their properties. Using SBGN-PD examples, we illustrate their interpretations, such as *zoom-out* and *zoom-in* details within a biochemical reaction network, and distinguishing networks of different types. Section 4 forms the heart of our formal development. In Subsection 4.1, we construct a category of process networks, and prove that it contains all finite colimits. We also compare our framework with the notion of a Petri net with link, a notion recently introduced by Aduddell et al in [1] for modelling regulatory networks. We start Subsection 4.2 by introducing the notion of an *open process network* or a *process network with an interface* using the Baez et al.’s theory of structured cospans [6]. Then, using the results from Subsection 4.1, we construct a symmetric monoidal double category whose horizontal 1-morphisms are open process networks. Furthermore, we make a pair of observations that enable us to illustrate various elements in the above symmetric monoidal double category with concrete examples visualised in SBGN-PD. In Subsection 4.3, we introduce the notion of a *process subnetwork of a process network* and its *environment*. Next, we introduce a tool that we call a *macroscope of a process subnetwork with respect to a network*. This notion allows us to study the influence of the process subnetwork on its environment and vice versa. We end the Section 4 by applying our above said macroscope on a standard SBGN-PD. In Section 5, we develop formal methods to translate a generic SBGN-PD into a process network. These formal translation methods allow us to use the mathematical theory developed in Section 3 and Section 4 to apply on a generic biochemical reaction network that admits an SBGN-PD visualisation. Finally, in Section 6, We conclude our manuscript with a concise summary of our main results and a brief discussion of potential future directions.

2 An illustration of our results by the way of examples

This section attempts to illustrate the main achievements of this manuscript through some standard examples of biochemical reaction networks visualised in SBGN Process Description. We postpone our concrete theoretical development until Section 3.

We begin our treatment with an example of a biochemical reaction visualised as an SBGN Process Description (Figure 1 (top)), and the visualisation of its formal abstraction (Figure 1 (bottom)), as done in our framework in the later sections. The reaction in Figure 1 (top) describes

the activation of the molecule ERK through phosphorylation (attaching a phosphate group P). The process requires energy generated by breaking down ATP, thereby releasing ADP. The activation of ERK is facilitated by the phosphorylated MEK. In SBGN Process Descriptions, *entity pool nodes* like macromolecules and simple chemicals are visualised by rectangular glyphs with rounded corners and circles respectively. The small inserted circles visualise covalent modifications (like the state of phosphorylations), and the small squares represent process nodes describing biochemical processes. A connecting arc between a biochemical entity and the process node denotes *consumption*, a connecting arc (from the process node to a biochemical entity) with a black arrowhead represents *production* and a connecting arc (from a biochemical entity to the process node) with a small white circular head denotes *catalysis*.

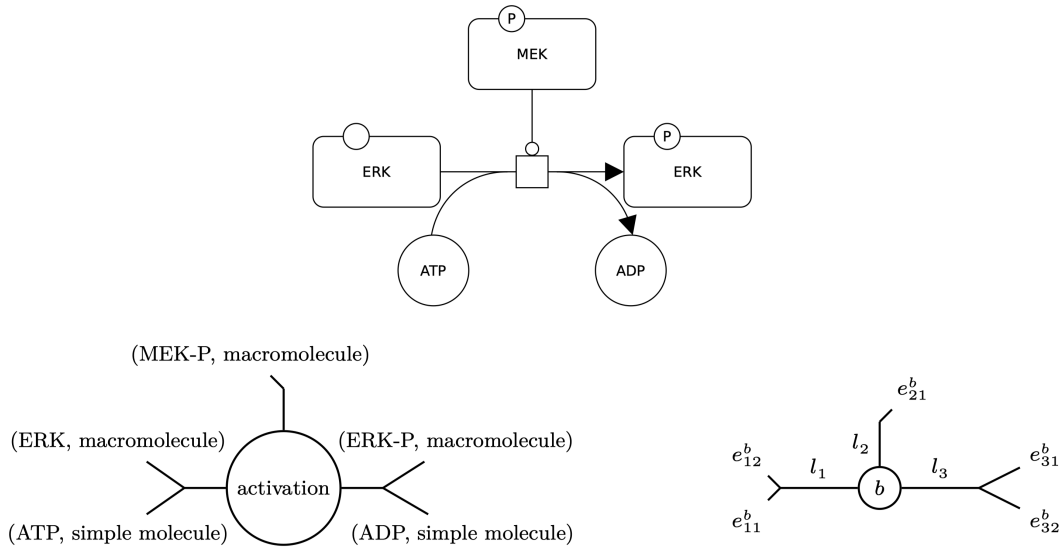


Figure 1: Example of an SBGN Process Description describing a biochemical reaction (top), and the visualisation of its formal abstraction (bottom right) as done in our framework (Definition 3.1). In the bottom left, we illustrate the formal translation of the SBGN-PD to its abstraction as discussed in Example 3.4, and formally explained in Section 5.

The formal abstraction of SBGN-PD diagram, which we will define mathematically as a *process species* in Definition 3.1, is visualised in the bottom right of Figure 1. The process is drawn a circle, labelled b , and the arcs labelled l_1, l_2 and l_3 model consumption, catalysis and production, respectively, of the process b . Symbols e_{11}^b, e_{12}^b model respectively the simple chemical ATP and the macromolecule ERK, and are attached to the arc labelled l_1 . The symbol e_{21}^b models the macromolecule phosphorylated MEK which is attached to l_2 . Symbols e_{31}^b and e_{32}^b model the macromolecule phosphorylated ERK and the simple chemical ADP, respectively, and are attached to l_3 . Furthermore, observe that the attachment of biochemical entities to arcs like l_1, l_2 and l_3 are shown with additional arcs. In the bottom left of Figure 1, we illustrate the translation of the SBGN-PD (Figure 1 top) to our formal abstraction (bottom right of Figure 1). Example 3.4 discusses such translation, and Section 5 explains it formally.

Our theoretical framework (Section 3 and Section 4) provides us with organisational principles (as discussed in Section 1) for biochemical reaction networks admitting SBGN-PD visualisations. We achieve such organisational principles through our two main results in this manuscript. Precisely, through Theorem 4.12 we get (i) formal ways to compose a collection of biochemical molecular/cellular networks into a composite network and decompose a large network into smaller sub-components, (ii) formal ways to zoom in and zoom out details in a biochemical molecular/cellular network, (iii) formal compatibility features between the said compositionality and the said process of zooming-out and zooming-in details. The formal study of how a particular portion of a network depends on the entities produced outside it, and conversely, how the network outside this particular portion depends on the entities produced inside the said portion, we obtain through Definition 4.24.

2.1 An illustration of Theorem 4.12

In technical terms, Theorem 4.12 produces a symmetric monoidal double category whose horizontal 1-morphisms can be interpreted as SBGN Process Descriptions, and 2-morphisms can be interpreted as zoom-out or zoom-in operations on the details of a biochemical network visualised using a SBGN-PD. The composition laws and the monoidal product laws in the constructed symmetric monoidal double category provide us with a compositional framework for SBGN-PD which remain compatible with our zoom-in and zoom-out operations.

In Figure 2, we illustrate how to build an SBGN-PD visualisation of the MAPK cascade by composing three reaction networks ((a), (b) and (c)) and two reaction networks ((d) and (e)) using our Theorem 4.12. The dotted black lines denote compositions (interconnections).

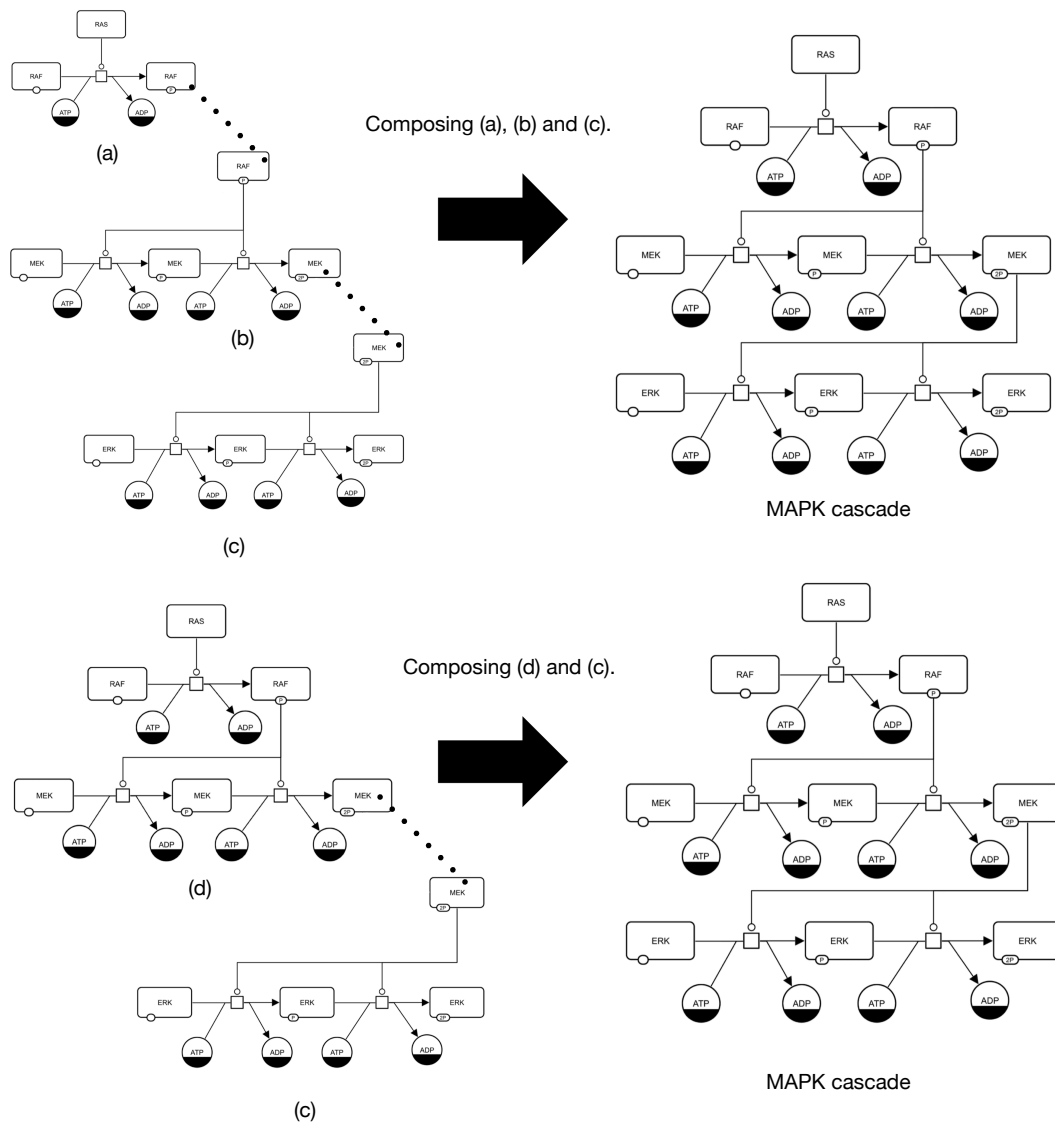


Figure 2: Illustration of building an SBGN-PD visualisation of the MAPK cascade by composing three reaction networks (a), (b) and (c), and two reaction networks (d) and (e), using the Theorem 4.12. SBGN images are derived from the MAPK cascade example on Page 65 in [35].

We can also formally compose (using the Theorem 4.12) the SBGN visualisation of the whole MAPK cascade with other biochemical networks to form a larger network, as visualized in Figure

3. Here, we demonstrate how to build insulin-like Growth Factor (IGF) signalling by composing the SBGN-PD visualisation of the MAPK cascade with two other biochemical molecular networks (marked with blue and grey) using our Theorem 4.12. The dotted black lines denote compositions (interconnections). However, while visualizing the IGF signalling using SBGN, usually an *encapsulation node* called the *submap* is used to hide the details of the MAPK cascade in the pathway, as shown in Figure 5. Here, the *reference nodes tags* show how the submap is connected to the rest part of the IGF signalling via the macromolecules RAS and ERK through *equivalence arcs* (connecting the RAS and the tag RAS, and the ERK and the tag ERK).

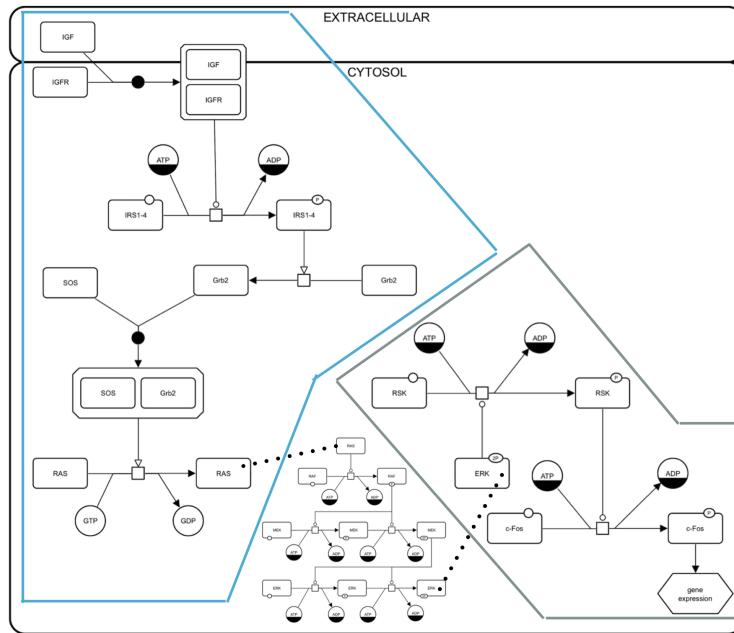


Figure 3: An illustration of building an SBGN-PD visualisation of the Insulin-like Growth Factor (IGF) signalling by composing the MAPK cascade with two other biochemical molecular networks (marked in blue and grey) using the Theorem 4.12. SBGN images are derived from IGF signalling and MAPK cascade examples on Pages 64 and 65 in [35].

Observe that in Figure 3, we encounter some geometric shapes such as the ones highlighted in Figure 4. According to SBGN PD language Level 1 Version 2.0 as in [35], we now briefly explain their meanings. The geometric shape Figure 4(a) represents the process node *association*. For example, in Figure 3, the macromolecules IGF and IGFR combine to form a *complex* through association.

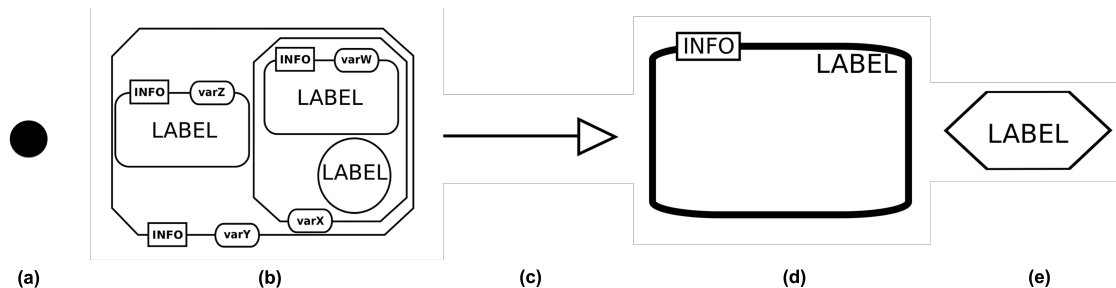


Figure 4: Some geometric shapes used in Figure 3. Here, (a), (b), (c), (d) and (e), respectively, denote association, complex node, stimulation arc, compartment node and phenotype. SBGN images are derived from the reference card on Page 75 in [35].

The geometric shape Figure 4(b) denotes a *complex node*, a biochemical entity comprising other biochemical entities like macromolecules, simple chemicals, multimers, or other complexes, connected by non-covalent bonds. In SBGN Process Descriptions, the stimulation of a process by a biochemical entity is denoted by a connecting arc (from an entity to the process node) with a white arrowhead (see Figure 4(c)). For example, in Figure 3, the macromolecule IRS1-4 stimulates the activation of the macromolecule Grb2. In SBGN, the geometric shape Figure 4(d) denotes a *compartment node*, representing a logical or physical structure. Every entity pool node, such as macromolecule, simple chemical, complex, etc., belongs to a compartment. Two identical entity pool nodes located in different compartments are considered different entities. In Figure 3, two compartments are used: extracellular and cytosol. In SBGN, geometric shape Figure 4(e) denotes a *phenotype*. In Figure 3, we have the phenotype gene transcription.

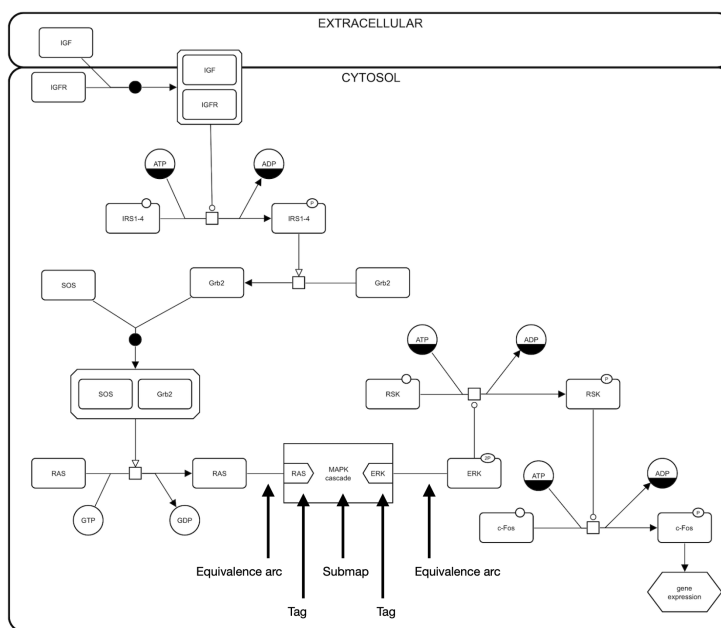


Figure 5: An illustration of the encapsulation node submap, the reference node tag and the equivalence arc in the SBGN-PD visualisation of the IGF signalling. The SBGN image is taken from the example of IGF signalling on Page 64, [35].

Often to study complicated biochemical reaction networks, we purposefully omit details to obtain a broader view of the whole reaction network. Our Theorem 4.12 provides us with a formal way to forget details from biochemical reaction networks such that the forgetting procedure (zooming-out procedure) is compatible with our formal compositional framework, as is illustrated in Figure 6. Here, we start with the SBGN-PD visualisations of two biochemical reactions numbered Figure 6(1) and Figure 6(2). Our Theorem 4.12 allows us to zoom-out (shown with the thin black arrows) by forgetting ADP's and ATP's from the reactions, and in turn, we obtain the reactions Figure 6(3) from Figure 6(1), and Figure 6(4) from Figure 6(2). Then, again the Theorem 4.12 let us combine Figure 6(3) and Figure 6(4) to obtain the reaction network Figure 6(6), and combine the reactions Figure 6(1) and Figure 6(2) to get the reaction network Figure 6(5). More interestingly, Theorem 4.12 provides us with a canonical way of combining two zooming-out procedures (Figure 6(1) to Figure 6(3) and Figure 6(2) to Figure 6(4)) such that the combined zoom-out procedure is compatible with the composition process. More precisely, here, the combined zoom-out process takes the reaction network Figure 6(5) to the reaction network Figure 6(6). Here, the dotted lines denote compositions. We provide the technical details of the above-mentioned procedure in Example 4.18.

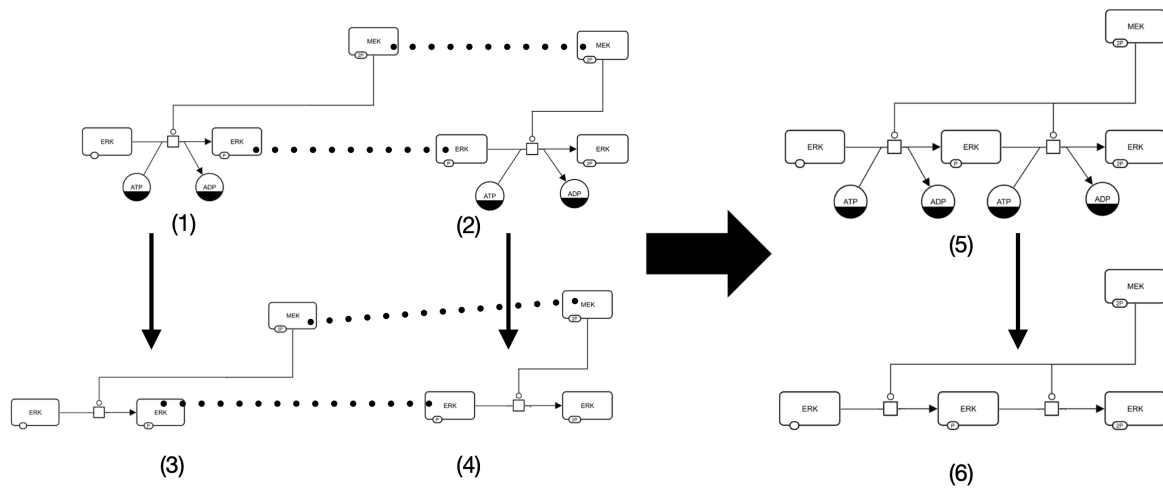


Figure 6: An illustration of formally zooming-out details in a biochemical reaction network using the Theorem 4.12. This figure, in particular, demonstrates how Theorem 4.12 provides a compatibility between the formal zooming-out methods and the compositionality. SBGN images are derived from the MAPK cascade example on Page 65, [35].

2.2 An illustration of Definition 4.24

Often, especially for disease-related purposes, it is essential to see how a particular portion of a biochemical network gets affected by the remaining part of the network and the converse i.e. how that particular portion affects the rest of the network. We introduce a mathematical technique called a *macroscope* (Definition 4.24), which allows us to formalise such effects. We choose the name *macroscope* because it allows us to see the overall effect of a biochemical reaction network on its surrounding network and vice versa. We illustrate the *macroscope* in Figure 7. In particular, if we apply the *macroscope* to the portion (marked in blue), then first it picks out the macromolecule phosphorylated RAF and the macromolecule double phosphorylated MEK. Then it tells the role they are playing. To be more precise, it says that the outer portion of the network is modulating (here catalysis) the blue portion via phosphorylated RAF and on the other hand, the blue portion is modulating (here catalysis) the outer portion of the network through double phosphorylated MEK. We provide the technical details of the above technique in Figure 21.

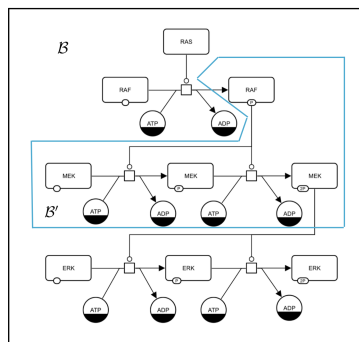


Figure 7: An illustration of the *macroscope*, formally introduced in Definition 4.24. Applying the *macroscope* in the blue marked portion, we can conclude that the outer portion is catalysing the blue marked portion through the phosphorylated RAF, and in turn, the blue marked portion is catalysing the outer portion through the double phosphorylated MEK. The SBGN image is taken from the MAPK cascade example on Page 65 in [35].

3 Process species, process networks, and their transformations

This section introduces mathematical structures called *process species*, *process network* and *morphisms of process networks*, which model, respectively, a biochemical reaction, biochemical reaction network and a process of transforming a biochemical reaction network into another.

3.1 Process networks and process species

Definition 3.1 (Process network and process species). Let $\bar{\mathbb{Z}}_2$ be the commutative monoid whose underlying set is $\{0, 1\}$ and the identity is 0 with respect to the binary operation given as $x + y := \max\{x, y\}$ for all $x, y \in \{0, 1\}$. Then, a *process network* \mathcal{B} consists of the following:

- A set B , whose elements b are called *process species*.
- A set E , whose elements e are called *entities*.
- A set of functions $\mathcal{L} := \{l_i: B \rightarrow \bar{\mathbb{Z}}_2[E]\}_{i \in \{1, 2, \dots, n\}}$, where $\bar{\mathbb{Z}}_2[E]$ is the free commutative monoid on the set E with the coefficients from $\bar{\mathbb{Z}}_2$.

We say \mathcal{B} is *process network on the set E with n legs l_1, l_2, \dots, l_n* and is denoted as $(E, B, \{l_i\}_n)$. We call $l_i(b)$ as the *i -th leg of the process species b* . We say that the *i -th leg of the process species b is missing* if $b_{\text{legs}}(l_i) = 0$.

Definition 3.2 (Evaluation function of a process species). Given a process network $(E, B, \{l_i\}_n)$, for any process species $b \in B$, we will call the function $b_{\text{legs}}: \mathcal{L} \rightarrow \bar{\mathbb{Z}}_2[E], l_i \mapsto l_i(b)$, the *evaluation function of the process species b* , where $\mathcal{L} = \{l_1, l_2, \dots, l_n\}$.

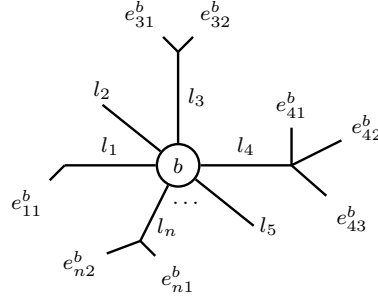


Figure 8: Evaluation function $b_{\text{legs}}: \mathcal{L} \rightarrow \bar{\mathbb{Z}}_2[E]$ for a process species b . Observe that we draw the legs $l_2, l_5, l_6, \dots, l_{n-1}$, which are evaluated zero at b , but we do not attach entities to them.

Remark 3.3. Consider a process network $\mathcal{B} = (E, B, \{l_i\}_n)$. Observe that for any $b \in B$ and $i \in \{1, 2, \dots, n\}$ such that $l_i(b) \neq 0$, there is a unique way to write $l_i(b) = \sum_{j=1}^{m_b^i} e_{ij}^b$ with distinct non-zero summands, where $m_b^i \in \mathbb{N}$ and $e_{ij}^b \in E$. Let us denote the set $\{e_{ij}^b: l_i(b) = \sum_{j=1}^{m_b^i} e_{ij}^b\}$ as $\bar{e}_{i,b}$. Note that $|\bar{e}_{i,b}| = m_b^i$, where $|\bar{e}_{i,b}|$ denotes the cardinality of the set $\bar{e}_{i,b}$. When $l_i(b) = 0$, we define $\bar{e}_{i,b}$ as the empty set \emptyset .

A general element x in $\bar{\mathbb{Z}}_2[E]$ is a formal linear combination of the form $x = \alpha_1 e_1 + \alpha_2 e_2 + \dots + \alpha_n e_n$, where $\alpha_i \in \bar{\mathbb{Z}}_2$ and $e_i \in E$ for all $i = 1, 2, \dots, n$ and $n \in \mathbb{N}$. Thus, we define the evaluation

function b_{legs} for Figure 8 as

$$\begin{aligned}
b_{\text{legs}}(l_1) &= 1 \cdot e_{11}^b + \left(\sum_{e \in (E - \{e_{11}^b\})} 0 \cdot e \right) = e_{11}^b \\
b_{\text{legs}}(l_2) &= \left(\sum_{e \in E} 0 \cdot e \right) = 0 \\
b_{\text{legs}}(l_3) &= 1 \cdot e_{31}^b + 1 \cdot e_{32}^b + \left(\sum_{e \in (E - \{e_{31}^b, e_{32}^b\})} 0 \cdot e \right) = e_{31}^b + e_{32}^b \\
b_{\text{legs}}(l_4) &= 1 \cdot e_{41}^b + 1 \cdot e_{42}^b + 1 \cdot e_{43}^b + \left(\sum_{e \in (E - \{e_{41}^b, e_{42}^b, e_{43}^b\})} 0 \cdot e \right) = e_{41}^b + e_{42}^b + e_{43}^b \\
b_{\text{legs}}(l_k) &= \left(\sum_{e \in E} 0 \cdot e \right) = 0 \text{ for all } k = 5, 6, \dots, n-1 \\
b_{\text{legs}}(l_n) &= 1 \cdot e_{n1}^b + 1 \cdot e_{n2}^b + \left(\sum_{e \in (E - \{e_{n1}^b, e_{n2}^b\})} 0 \cdot e \right) = e_{n1}^b + e_{n2}^b
\end{aligned} \tag{3.1}$$

In Equation (3.1), the coefficient 1 and 0 expresses, respectively, the presence and absence of the entities. For example, the expression $b_{\text{legs}}(l_3) = e_{31}^b + e_{32}^b$ says that the only entities that are associated to the leg l_3 of the process species b are e_{31}^b and e_{32}^b . Our definition of process network is motivated by the definition of a Petri net as in [7]. However, the above definition is tailored to our purpose. There are two main differences in our definition. First, instead of just a pair of maps (source and target), we have room for more maps $\{l_i\}_n$ to consider modulators like stimulation, catalysis, inhibition, necessary stimulation, etc. Secondly, the maps $\{l_i\}_n$ are valued in $\bar{\mathbb{Z}}_2[E]$ instead of $\mathbb{N}[E]$. This emphasises the fact that often one cannot quantify the exact number of molecules involved in a reaction. In that case, one only measures the presence or absence, and assumes that the presence means presence in abundance. To take account of it, in SBGN visualisation of a biochemical reaction network, precise stoichiometry is absent. With this motivation, in our framework, we consider only the presence or absence of entities given by the coefficients 1 and 0, respectively, coming from the commutative monoid $\bar{\mathbb{Z}}_2$.

Example 3.4 (A process network with one process species). In Figure 1, we consider the SBGN-PD visualisation of the biochemical reaction, where a molecule MEK-P modulates the activation of ERK into ERK-P. Using notations from Definition 3.1, we construct an associated process network $\mathcal{B} = (E, B, \{l_i\}_3)$ as follows:

- $B := \{b\}$, the singleton set containing the process species.
- \mathcal{L} has three elements l_1, l_2, l_3 , representing consumption arc, modulation arc and production arc, respectively, in Figure 1.
- $E := \{e_{11}^b, e_{12}^b, e_{21}^b, e_{31}^b, e_{32}^b\}$, where
 - $e_{11}^b = (\text{ATP, simple chemical})$,
 - $e_{12}^b = (\text{ERK, macromolecule})$,
 - $e_{21}^b = (\text{MEK-P, macromolecule})$,
 - $e_{31}^b = (\text{ERK-P, macromolecule})$,
 - $e_{32}^b = (\text{ADP, simple chemical})$.

If we represent the *set of molecules* $\{\text{MEK-P, ERK, ERK-P, ATP, ADP}\}$ by M and the *set of types of molecules involved* $\{\text{macromolecule, simple chemical}\}$ by T , then the set $E = M \times T$.

- Legs $l_1, l_2, l_3: B \rightarrow \bar{\mathbb{Z}}_2[E]$ are defined as $b \mapsto e_{11}^b + e_{12}^b$, $b \mapsto e_{21}^b$ and $b \mapsto e_{31}^b + e_{32}^b$, respectively.

Hence, $\mathcal{B} = (E, B, \{l_i\}_3)$ defines a process network on the set E with three legs. Comparing with Figure 8, observe that the bottom right diagram in Figure 1 describes the evaluation function $b_{\text{legs}}: \mathcal{L} \rightarrow \bar{\mathbb{Z}}_2[E]$ of the process species b .

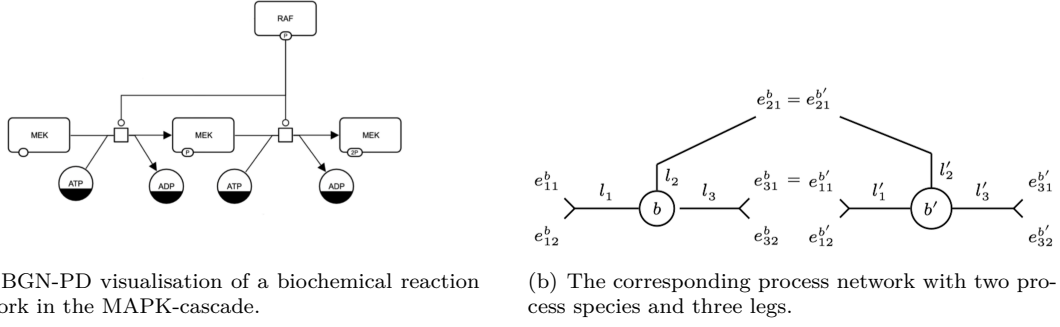


Figure 9: A biochemical reaction network as a process network. The SBN image is derived from the MAPK cascade example on Page 65, [35].

Example 3.5 (A process network with two process species). In SBN visualisation of biochemical reaction networks, the entity pool nodes that can appear multiple times are called *clone makers* and are distinguished by dark bands along their bottoms. For example, in Figure 9(a), simple chemicals ADP and ATP appear two times in the SBN-PP visualisation and hence are clone makers. However, for a technical reason needed later in this paper, while modelling SBN visualisations as process networks, we will distinguish between the same entity pool nodes appearing multiple times as clone makers. For example, while describing the SBN-PP in Figure 9(a) as a process network, we will distinguish between the ADP associated to the left process node and the ADP associated to the right process node. Below, we describe the process network $\mathcal{B} = (E, B, \{l_i\}_3)$ associated to the SBN-PP visualisation in Figure 9(a):

- $B := \{b, b'\}$ is a two element set containing the pair of process nodes in Figure 9(a) such that b and b' represent the left and right process nodes respectively.
- \mathcal{L} has three elements l_1, l_2, l_3 , representing consumption arc, modulation arc and production arc, respectively, in Figure 9(a).
- $E := \{e_{11}^b, e_{12}^b, e_{21}^b, e_{31}^b, e_{32}^b\} \cup \{e_{11}^{b'}, e_{12}^{b'}, e_{21}^{b'}, e_{31}^{b'}, e_{32}^{b'}\}$ (see Figure 9(b)), where
 - $e_{11}^b = (\text{MEK}, \text{macromolecule})$,
 - $e_{12}^b = (\text{ATP}_b, \text{simple chemical})$,
 - $e_{21}^b = (\text{RAF-P}, \text{macromolecule})$,
 - $e_{31}^b = (\text{MEK-P}, \text{macromolecule})$,
 - $e_{32}^b = (\text{ADP}_b, \text{simple chemical})$,
 - $e_{11}^{b'} = (\text{MEK-P}, \text{macromolecule}) = e_{31}^b$,
 - $e_{12}^{b'} = (\text{ATP}_{b'}, \text{simple chemical})$,
 - $e_{21}^{b'} = (\text{RAF-P}, \text{macromolecule}) = e_{21}^b$,
 - $e_{31}^{b'} = (\text{MEK-2P}, \text{macromolecule})$,
 - $e_{32}^{b'} = (\text{ADP}_{b'}, \text{simple chemical})$.

Here, the notations RAF-P, MEK-P, MEK-2P denote the phosphorylated RAF, phosphorylated MEK and double phosphorylated MEK, respectively. Also, by using the notation ATP_b and $\text{ATP}_{b'}$, we mathematically distinguish between the biologically same molecule ATP appearing as clone makers in Figure 9(a). We do the same for the molecule ADP.

- Legs $l_1, l_2, l_3: B \rightarrow \bar{\mathbb{Z}}_2[E]$ are defined respectively, as
 - $b \mapsto e_{11}^b + e_{12}^b, b' \mapsto e_{11}^{b'} + e_{12}^{b'}$,
 - $b \mapsto e_{21}^b, b' \mapsto e_{21}^{b'}$,
 - $b \mapsto e_{31}^b + e_{32}^b, b' \mapsto e_{31}^{b'} + e_{32}^{b'}$.

$\mathcal{B} = (E, B, \{l_i\}_3)$ is a process network on E with three legs.

3.2 Transforming a process network into another: Morphisms of process networks

Here, we introduce the notion of a morphism of process networks and illustrate how it models the process of transforming a biochemical reaction network into another.

Definition 3.6 (Morphism of process networks). For a fixed $n \in \mathbb{N}$, a *morphism from a process network* $\mathcal{B} = (E, B, \{l_i\}_n)$ to another process network $\mathcal{B}' = (E', B', \{l'_i\}_n)$ is given by a pair of functions $F := (\alpha: E \rightarrow E', \beta: B \rightarrow B')$, such that following diagram commutes for all $i \in \{1, 2, 3, \dots, n\}$, where $\bar{\mathbb{Z}}_2[\alpha]: \bar{\mathbb{Z}}_2[E] \rightarrow \bar{\mathbb{Z}}_2[E']$ is the unique monoid homomorphism extending α .

$$\begin{array}{ccc} B & \xrightarrow{l_i} & \bar{\mathbb{Z}}_2[E] \\ \downarrow \beta & & \downarrow \bar{\mathbb{Z}}_2[\alpha] \\ B' & \xrightarrow{l'_i} & \bar{\mathbb{Z}}_2[E'] \end{array}$$

Next, we show how the evaluation functions of process species (Definition 3.2) behaves with the morphisms of process networks. We will see how their behaviour provides us with formal criteria for distinguishing between reactions with the modulator's influence and the ones without such influences.

Lemma 3.7. Let $\mathcal{B} = (E, B, \{l_i\}_n)$ and $\mathcal{B}' = (E', B', \{l'_i\}_n)$ be a pair of process networks. Then, for any morphism $F = (\alpha, \beta): \mathcal{B} \rightarrow \mathcal{B}'$ we have the following conditions:

- (a) if $b_{\text{legs}}(l_i) = 0$, then $\beta(b)_{\text{legs}}(l'_i) = 0$,
- (b) if $b_{\text{legs}}(l_i) \neq 0$, then $\beta(b)_{\text{legs}}(l'_i) \neq 0$,
- (c) if $b_{\text{legs}}(l_i) \neq 0$, then using the notations introduced in Remark 3.3, we have $|\bar{e}_{i,b}| \geq |\bar{e}_{i,\beta(b)}|$,

for each $b \in B$ and $i \in \{1, 2, \dots, n\}$, where b_{legs} and $\beta(b)_{\text{legs}}$ are the evaluation functions (see Definition 3.2) of the process species b and $\beta(b)$ respectively.

Proof. The proof follows directly from the Definition 3.6 itself. \square

Example 3.8. Consider process networks $\mathcal{B} = (E = \{e_1, e_2, e_3, e_4, e_5, e_6\}, B = \{b_1, b_2\}, \{l_i\}_3)$, $\mathcal{B}' = (E = \{e'_1, e'_2, e'_3, e'_4\}, B' = \{b'\}, \{l'_i\}_3)$ and $\bar{\mathcal{B}} = (E = \{\bar{e}_1, \bar{e}_2\}, B = \{\bar{b}\}, \{\bar{l}_i\}_3)$, where for each $i \in \{1, 2, 3\}$, l_i, l'_i, \bar{l}_i are as shown in Figure 10. Observe that as a consequence of the condition (a) in the Lemma 3.7, there cannot exist a morphism of process networks from \mathcal{B} to \mathcal{B}' and from $\bar{\mathcal{B}}$ to \mathcal{B}' . Furthermore, there cannot exist any morphism from \mathcal{B}' to \mathcal{B} and from \mathcal{B}' to $\bar{\mathcal{B}}$ due to condition (b) in the Lemma 3.7. In the context of biochemical molecular networks, one can interpret them as a formal way to distinguish between biochemical reactions without the modulator's influence and reactions with the modulator's influence. Here, the reaction modelled in \mathcal{B}' has an influence of the modulator e , whereas all the reactions modelled in \mathcal{B} and $\bar{\mathcal{B}}$ have no influence of modulators.

Example 3.9. Let us consider process networks $\mathcal{B} = (E, B, \{l_i\}_3)$, $\bar{\mathcal{B}} = (\bar{E}, \bar{B}, \{\bar{l}_i\}_3)$, $\mathcal{B}' = (E', B', \{l'_i\}_3)$ and $\bar{\mathcal{B}}' = (\bar{E}', \bar{B}', \{\bar{l}'_i\}_3)$, where $E := \{e_1, e_2, e_3, e_4, e_5, e_6\}$, $\bar{E} := \{e_2, e_5, e_6\}$, $E' := \{e'_1, e'_2, e, e'_3, e'_4\}$, $\bar{E}' := \{e'_1, e, e'_3\}$, $B := \{b_1, b_2\}$, $\bar{B} := \{b_2\}$, $B' := \{b'\}$, $\bar{B}' := \{b'\}$ (see Figure 11). Define $F := (\alpha: E \rightarrow \bar{E}, \beta: B \rightarrow \bar{B})$, where $\alpha: E \rightarrow \bar{E}$ is given by $e_1 \mapsto e_6, e_2 \mapsto e_2, e_3 \mapsto e_5, e_4 \mapsto e_5, e_5 \mapsto e_5, e_6 \mapsto e_6$ and $\beta: B \rightarrow \bar{B}$ is given as $b_1 \mapsto b_2, b_2 \mapsto b_2$. Now, define $\bar{F} := (\bar{\alpha}: \bar{E} \rightarrow E, \bar{\beta}: \bar{B} \rightarrow B)$, where $\bar{\alpha}: \bar{E} \rightarrow E$ is given as $e_2 \mapsto e_2, e_6 \mapsto e_6, e_5 \mapsto e_5$ and $\bar{\beta}: \bar{B} \rightarrow B$ is given by $b_2 \mapsto b_2$. Defining $F' := (\alpha': E' \rightarrow \bar{E}', \beta': B' \rightarrow \bar{B}')$, where $\alpha': E' \rightarrow \bar{E}'$ is defined as $e'_1 \mapsto e'_1, e'_2 \mapsto e'_1, e'_3 \mapsto e'_3, e'_4 \mapsto e'_3, e \mapsto e$ and $\beta': B' \rightarrow \bar{B}'$ is defined by $b' \mapsto b'$. From the evaluation functions shown in Figure 11, it is straightforward to verify that F, \bar{F} and F' are morphisms of process networks. Observe in Figure 11 that one can interpret morphisms $F: \mathcal{B} \rightarrow \bar{\mathcal{B}}$ and $F': \mathcal{B}' \rightarrow \bar{\mathcal{B}}'$ as ways of zooming-out details, and the morphism $\bar{F}: \bar{\mathcal{B}} \rightarrow \mathcal{B}$ as a way to zoom-in details in biochemical reaction networks. An SBGN-PD visualisation of the zooming-out procedure is modelled at the bottom of the Figure 11, where F' models the process of forgetting ADP and ATP in the reaction describing the activation of the ERK molecule through phosphorylation. Also, one can check that as a consequence of the condition (c) in the Lemma 3.7, there can not exist a morphism of process network from $\bar{\mathcal{B}}'$ to \mathcal{B}' .

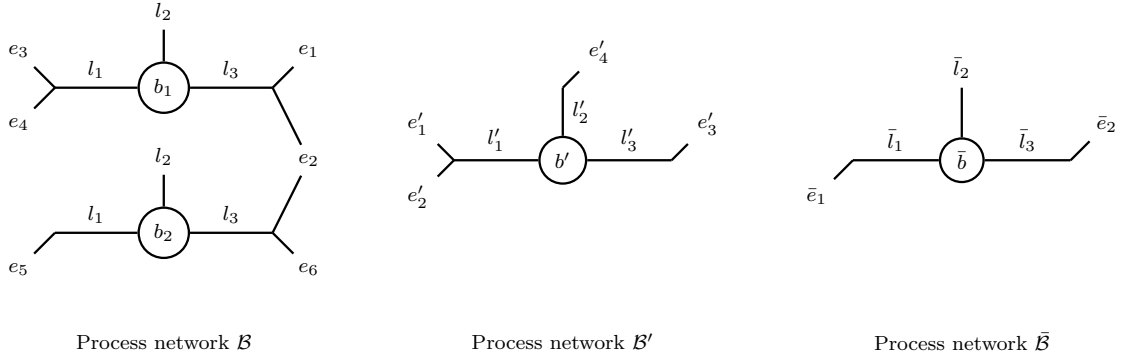


Figure 10: An illustration of condition (a) and condition (b) in Lemma 3.7, as discussed in Example 3.8. Due to (a), there cannot exist a morphism of process networks from \mathcal{B} to \mathcal{B}' and from $\bar{\mathcal{B}}$ to \mathcal{B}' , whereas (b) ensures that there cannot exist any morphism from \mathcal{B}' to \mathcal{B} and from \mathcal{B}' to $\bar{\mathcal{B}}$.

4 An organising principle for process networks

This section develops a mathematical theory that enables us to

- (a) introduce a notion of a *process network with an interface*,
- (b) derive a formal way to combine process networks with interfaces into a composite process network with an interface,
- (c) derive a formal way to transform a process network with an interface to another process network with an interface,
- (d) find a formal way to study the *influence of a process subnetwork on the remaining portion of the network* and vice versa.

By an **organizational principle for process networks**, we mean (a), (b), (c) and (d), and their interrelationships. To formalise (a), (b) and (c), first we will construct a finitely cocomplete category whose objects are process networks (Definition 3.1) and morphisms are morphisms of process networks (Definition 3.6) and then, we will build a symmetric monoidal double category whose horizontal 1-morphisms are structured cospans in the category of process networks. However, (d) will be formalised using a combinatorial argument.

4.1 Category of process networks

For a fixed number of legs, the collection of process networks and their morphisms forms a category as we see next.

Proposition 4.1. For any $n \in \mathbb{N}$, the collection of process networks forms a category $\mathbf{Process}_n$ whose

- objects are process networks $\mathcal{B} = (E, B, \{l_i\}_n)$;
- a morphism from a process network $\mathcal{B} = (E, B, \{l_i\}_n)$ to another process network $\mathcal{B}' = (E', B', \{l'_i\}_n)$ is given by a pair of functions $F := (\alpha: E \rightarrow E', \beta: B \rightarrow B')$, such that

$$\begin{array}{ccc}
 B & \xrightarrow{l_i} & \bar{\mathbb{Z}}_2[E] \\
 \downarrow \beta & & \downarrow \bar{\mathbb{Z}}_2[\alpha] \\
 B' & \xrightarrow{l'_i} & \bar{\mathbb{Z}}_2[E']
 \end{array}$$

commutes for all $i \in \{1, 2, 3, \dots, n\}$.

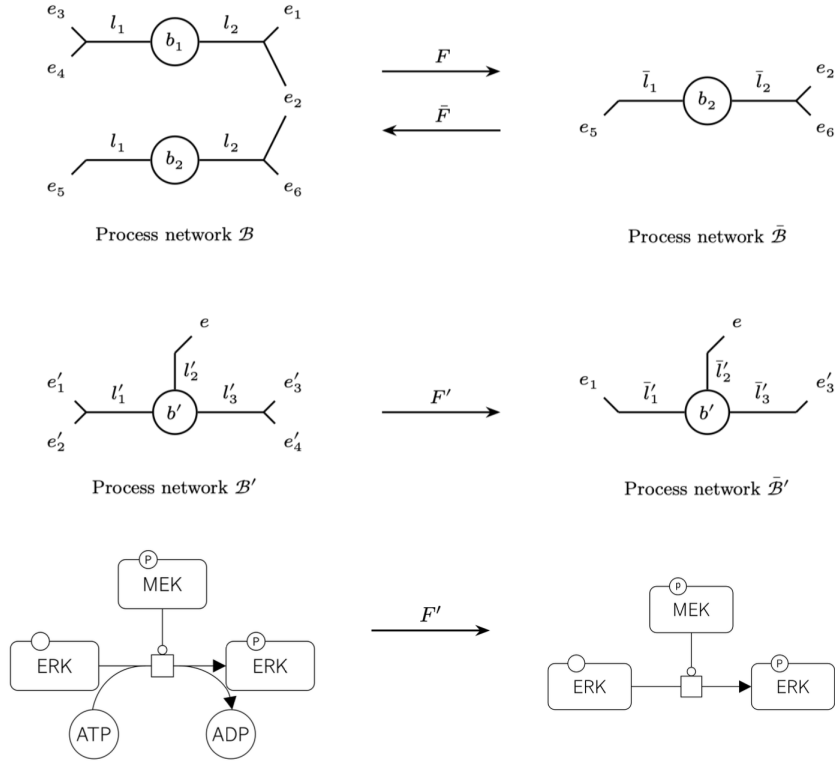


Figure 11: An illustration of Example 3.9, showing how to interpret morphisms of process networks as ways of ‘zooming-out and zooming-in details’ in biochemical reaction networks.

Proof. Let us consider a pair of morphisms $F: \mathcal{B} \rightarrow \mathcal{B}'$ and $G: \mathcal{B}' \rightarrow \mathcal{B}''$, defined as $F := (\alpha: E \rightarrow E', \beta: B \rightarrow B')$ and $G := (\alpha': E' \rightarrow E'', \beta': B' \rightarrow B'')$ where, $\mathcal{B} = (E, B, \{l_i\}_n)$, $\mathcal{B}' = (E', B', \{l'_i\}_n)$ and $\mathcal{B}'' = (E'', B'', \{l''_i\}_n)$. We define $G \circ F := (\alpha' \circ \alpha, \beta' \circ \beta)$. To see if the definition of $G \circ F$ makes sense, consider the diagrams

$$\begin{array}{ccc}
 B & \xrightarrow{l_i} & \bar{\mathbb{Z}}_2[E] \\
 \beta \downarrow & & \downarrow \bar{\mathbb{Z}}_2[\alpha] \\
 B' & \xrightarrow{l'_i} & \bar{\mathbb{Z}}_2[E'] \\
 \beta' \downarrow & & \downarrow \bar{\mathbb{Z}}_2[\alpha'] \\
 B'' & \xrightarrow{l''_i} & \bar{\mathbb{Z}}_2[E'']
 \end{array}$$

that commutes for all $i = \{1, 2, \dots, n\}$. Observe that from the commutativity of small squares, we have $l''_i \circ (\beta' \circ \beta) = \bar{\mathbb{Z}}_2[\alpha'] \circ \bar{\mathbb{Z}}_2[\alpha] \circ l_i$. Then, the observation $\bar{\mathbb{Z}}_2[\alpha' \circ \alpha] = \bar{\mathbb{Z}}_2[\alpha'] \circ \bar{\mathbb{Z}}_2[\alpha]$ concludes $G \circ F$ is well defined. For each object $\mathcal{B} = (E, B, \{l_i\}_n)$, it is easy to see that the identity morphism is given by $\text{id}_{\mathcal{B}} = (\text{id}: E \rightarrow E, \text{id}: B \rightarrow B)$. Finally, the associativity of composition follows from the associativity of the composition of functions. Hence, we proved **Process**_n is a category. \square

Now, since we will be representing process networks with interfaces as cospans in **Process**_n (Proposition 4.1), for composing cospans, we need the category **Process**_n to have all finite pushouts. In fact, we will show **Process**_n contains all finite colimits. For this, we proceed in two steps:

Step 1: We will show **Process**_n is equivalent to the comma category $\text{Id}/\bar{\mathbb{Z}}_2[-]^n$, where $\text{Id}: \mathbf{Set} \rightarrow \mathbf{Set}$ is the identity functor and $\bar{\mathbb{Z}}_2[-]^n: \mathbf{Set} \rightarrow \mathbf{Set}$ is the functor that takes a set E to the

set $\underbrace{\bar{\mathbb{Z}}_2[E] \times \bar{\mathbb{Z}}_2[E] \times \cdots \times \bar{\mathbb{Z}}_2[E]}_{n\text{-times}}$, and takes a function $\alpha: E \rightarrow E'$ to the function $\underbrace{\bar{\mathbb{Z}}_2[\alpha] \times \bar{\mathbb{Z}}_2[\alpha] \times \cdots \times \bar{\mathbb{Z}}_2[\alpha]}_{n\text{-times}}: \underbrace{\bar{\mathbb{Z}}_2[E] \times \bar{\mathbb{Z}}_2[E] \times \cdots \times \bar{\mathbb{Z}}_2[E]}_{n\text{-times}} \rightarrow \underbrace{\bar{\mathbb{Z}}_2[E'] \times \bar{\mathbb{Z}}_2[E'] \times \cdots \times \bar{\mathbb{Z}}_2[E']}_{n\text{-times}}$.

Step 2: We will show $\text{Id}/\bar{\mathbb{Z}}_2[-]^n$ has all finite colimits.

Lemma 4.2. $\mathbf{Process}_n$ is equivalent to the comma category $\text{Id}/\bar{\mathbb{Z}}_2[-]^n$.

Proof. First we show that the following functor is well defined:

$$\begin{aligned} F: \mathbf{Process}_n &\rightarrow \text{Id}/\bar{\mathbb{Z}}_2[-]^n \\ (E, B, \{l_i\}_n) &\mapsto (B, \prod_{i=1}^{i=n} l_i, E) \\ ((\alpha, \beta): (E, B, \{l_i\}_n) \rightarrow (E', B', \{l'_i\}_n)) &\mapsto (\beta: B \rightarrow B', \alpha: E \rightarrow E'). \end{aligned} \quad (4.1)$$

Let us denote the maps induced by F on objects and morphism using the notation F_0 and F_1 , respectively. From the definition of the function

$$\prod_{i=1}^{i=n} l_i: B \rightarrow \underbrace{\bar{\mathbb{Z}}_2[E] \times \bar{\mathbb{Z}}_2[E] \times \cdots \times \bar{\mathbb{Z}}_2[E]}_{n\text{-times}}, b \mapsto (l_1(b), l_2(b), \dots, l_n(b)),$$

it follows F_0 is well-defined. To see F_1 is well-defined, we need to show that

$$(\beta, \alpha) \in \text{hom}_{\text{Id}/\bar{\mathbb{Z}}_2[-]^n} \left((B, \prod_{i=1}^{i=n} l_i, E), (B', \prod_{i=1}^{i=n} l'_i, E') \right).$$

Now, observe that for our purpose it is sufficient to prove the commutativity of the following diagram

$$\begin{array}{ccc} B & \xrightarrow{\prod_{i=1}^{i=n} l_i} & \bar{\mathbb{Z}}_2[E]^n \\ \beta \downarrow & & \downarrow \bar{\mathbb{Z}}_2[-]^n(\alpha) \\ B' & \xrightarrow{\prod_{i=1}^{i=n} l'_i} & \bar{\mathbb{Z}}_2[E']^n \end{array}$$

for all $i \in \{1, 2, \dots, n\}$. Then, for each i , the commutativity of the following diagrams

$$\begin{array}{ccc} B & \xrightarrow{l_i} & \bar{\mathbb{Z}}_2[E] \\ \beta \downarrow & & \downarrow \bar{\mathbb{Z}}_2[\alpha] \\ B' & \xrightarrow{l'_i} & \bar{\mathbb{Z}}_2[E'] \end{array}$$

implies

$$\prod_{i=1}^{i=n} (\bar{\mathbb{Z}}_2[\alpha] \circ l_i) = \prod_{i=1}^{i=n} (l'_i \circ \beta) \quad (4.2)$$

It is easy to see that the left hand side of 4.2 is same as $\bar{\mathbb{Z}}_2[-]^n(\alpha) \circ \prod_{i=1}^{i=n} l_i$ and the right hand side of 4.2 is same as $\prod_{i=1}^{i=n} l'_i \circ \beta$. Hence, F_1 is well-defined. Observe that from the definition of F itself (4.1), it is clear that F is a faithful functor. The fullness follows directly from the pointwise definition of 4.2. To show that F is essentially surjective, consider an object (B, f, E) in $\text{Id}/\bar{\mathbb{Z}}_2[-]^n$. Since $s(f) = B$ and $t(f) = \bar{\mathbb{Z}}_2[E] \times \bar{\mathbb{Z}}_2[E] \times \cdots \times \bar{\mathbb{Z}}_2[E]$, it is clear that $f = \prod_{i=1}^{i=n} l_i$ for some functions $l_1, l_2, \dots, l_n: B \rightarrow \bar{\mathbb{Z}}_2[E]$. Observe that $(E, B, \{l_i\}_n)$ is an object of $\mathbf{Process}_n$ by the pointwise definition in 4.2. Also, it is clear from the definition of F (4.1), that $F((E, B, \{l_i\}_n)) = (B, f, E)$. Thus, we have shown F is surjective, and hence, essentially surjective. So, we proved that $\mathbf{Process}_n$ is equivalent to the category $\text{Id}/\bar{\mathbb{Z}}_2[-]^n$. \square

Proposition 4.3. $\mathbf{Process}_n$ contains all finite colimits.

Proof. It follows from the *Theorem 3, Section 5.2 of [36]* that whenever the categories A and B have finite colimits, $F: A \rightarrow C$ is a functor preserving such colimits and $G: B \rightarrow C$ is any functor, then the comma category F/G has finite colimits. Hence, the category $\text{Id}/\bar{\mathbb{Z}}_2[-]^n$ has all finite colimits. Since by Lemma 4.2, $\mathbf{Process}_n$ is equivalent to $\text{Id}/\bar{\mathbb{Z}}_2[-]^n$, $\mathbf{Process}_n$ contains also all finite colimits. \square

Proposition 4.4. Let $m, n \in \mathbb{N}$, such that $m < n$. Then, there is a full embedding from the category $\mathbf{Process}_m$ to the category $\mathbf{Process}_n$.

Proof. Proof directly follows from the fullness and faithfulness of the functor

$$i: \mathbf{Process}_m \rightarrow \mathbf{Process}_n$$

which takes a biochemical process network $(E, B, \{l_i\}_m)$ with m legs to a biochemical process network $(E, B, \{l_i\}_n)$ with n legs such that $l_k = 0$ for $k > m$. \square

Hence, if $m < n \in \mathbb{N}$, then the Proposition 4.4 identifies a process network having m legs $\mathcal{B} = (E, B, \{l_i\}_m)$ with a process network having n legs $\mathcal{B}' = (E, B, \{l_i\}_n)$, where $l_k: B \rightarrow \bar{\mathbb{Z}}_2[E]$ are zero functions for $k > m$, see Figure 12.

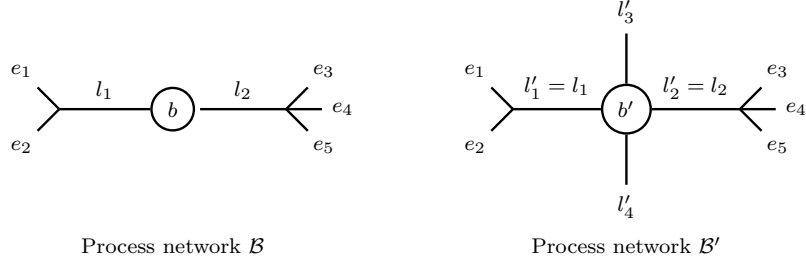
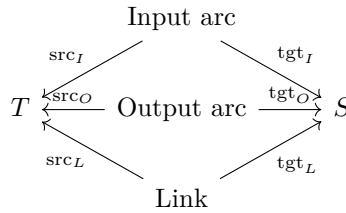


Figure 12: An illustration showing that the Proposition 4.4 allows us to treat the process network $\mathcal{B} = (E := \{e_1, e_2, e_3, e_4, e_5\}, B := \{b\}, \{l_i\}_2)$ as same to the process network $\mathcal{B}' = (E' := \{e_1, e_2, e_3, e_4, e_5\}, B' := \{b\}, \{l'_i\}_4)$ such that $l'_1 = l_1$, $l'_2 = l_2$, $l'_3 = 0$ and $l'_4 = 0$.

Remark 4.5 (Relation to Petri net with link). In [1], the authors defined a *Petri net with link* as a functor $P: \text{Sch}(\text{LPetri}) \rightarrow \mathbf{Set}$, where $\text{Sch}(\text{LPetri})$ is the category freely generated by the following morphisms:



Now, let us consider a subclass of Petri nets with links $P: \text{Sch}(\text{LPetri}) \rightarrow \mathbf{Set}$ which satisfy the following condition: For each $b \in P(T)$, the sets $P(\text{src}_I)(P(\text{tgt}_I)^{-1}(b))$, $P(\text{src}_L)(P(\text{tgt}_L)^{-1}(b))$, and $P(\text{tgt}_O)(P(\text{src}_O)^{-1}(b))$ are finite sets, and the functions $P(\text{src}_I): P(\text{Input arc}) \rightarrow P(S)$, $P(\text{src}_L): P(\text{Link}) \rightarrow P(S)$ and $P(\text{tgt}_O): P(\text{Output arc}) \rightarrow P(S)$ are injective functions. Then, it is lengthy but straightforward to show a one-one correspondence between such a subclass of Petri nets with links and the set of process networks with three legs.

4.2 Process networks with interfaces as structured cospans

To introduce the notion of a process network with an interface, we will borrow the theory of structured cospans as developed in [6]. To be more precise, we will use the theory of structured cospans to construct a symmetric monoidal double-category whose horizontal 1-morphisms are

process networks with interfaces. By an interface of a process network, we mean a set of entities (see Definition 3.1) associated to the process network through which the process network connects with other process networks. In mathematical terms, we will represent process networks with interfaces as structured cospans. For example, in the Figure 9, if we identify the pair of process species in the Figure 9(b), as a pair of process networks \mathcal{B} and \mathcal{B}' whose set of process species are respectively, $B_1 := \{b\}$ and $B_2 := \{b'\}$, then, observe that to build the SBGN visualisation of the biochemical reaction network in the Figure 9(a), we need to compose \mathcal{B} and \mathcal{B}' using an interconnection between the pair of entities e_{31}^b and $e_{11}^{b'}$ and the pair of entities e_{21}^b and $e_{21}^{b'}$. In this case, entities e_{31}^b and e_{21}^b lie in the interface of \mathcal{B} and the entities $e_{11}^{b'}$ and $e_{21}^{b'}$ lie in the interface of \mathcal{B}' . We begin our treatment by recalling the definition of a structured cospan.

Definition 4.6 (Section 2, [6]). Let C and X be a pair of categories. A *structured cospan* consists of a functor $L: C \rightarrow X$ along with a cospan in the category X of the following form:

$$\begin{array}{ccc} & x & \\ \mathcal{I} \nearrow & & \nwarrow \mathcal{O} \\ L(a) & & L(b) \end{array}$$

where a, b are objects of C and x is an object of X . Morphisms $\mathcal{I}: L(a) \rightarrow x$ and $\mathcal{O}: L(b) \rightarrow x$ are called the *left leg* and the *right leg* of the above structured cospan.

To obtain a notion of an interface of a process network using structured cospans, we in particular need to focus on a particular case, by constructing a functor $L: \mathbf{Set} \rightarrow \mathbf{Process}_n$ for each $n \in \mathbb{N}$. Using the notation \emptyset for both the empty set and the unique function between two empty sets, we state the following lemma.

Lemma 4.7.

$$\begin{aligned} L: \mathbf{Set} &\rightarrow \mathbf{Process}_n \\ E &\mapsto (E, \emptyset, \underbrace{\{\emptyset_{\bar{\mathbb{Z}}_2[E]}, \emptyset_{\bar{\mathbb{Z}}_2[E]}, \emptyset_{\bar{\mathbb{Z}}_2[E]}, \emptyset_{\bar{\mathbb{Z}}_2[E]}\}}_{n\text{-times}}) \\ (\alpha: E \rightarrow E') &\mapsto (\alpha, \emptyset) \end{aligned}$$

defines a functor, where $\emptyset_{\bar{\mathbb{Z}}_2[E]}: \emptyset \rightarrow \bar{\mathbb{Z}}_2[\mathbb{E}]$ is the canonical unique map.

Definition 4.8 (Open Process network). An *open process network* or a *process network with an interface* is defined as a structured cospan given by the functor $L: \mathbf{Set} \rightarrow \mathbf{Process}_n$ defined in Lemma 4.7 and a cospan in $\mathbf{Process}_n$ of the following form

$$\begin{array}{ccc} & \mathcal{B} & \\ \mathcal{I} \nearrow & & \nwarrow \mathcal{O} \\ L(X) & & L(Y) \end{array}$$

where X and Y are sets, and \mathcal{B} is a process network. We denote the above process network with an interface by the tuple $(\mathcal{B}, X, Y, \mathcal{I}, \mathcal{O})$. We will call the left leg \mathcal{I} and right leg \mathcal{O} as the *left interface* and the *right interface of the process network* \mathcal{B} .

Example 4.9. In Figure 13, we illustrate an open process network $(\mathcal{B}, \{1\}, \{2, 3\}, \mathcal{I}, \mathcal{O})$, where $\mathcal{B} = (\{e_{11}^b, e_{12}^b, e_{21}^b, e_{31}^b, e_{32}^b\}, \{b\}, \{l_i\}_3)$ is a process network with three legs l_1, l_2 , and l_3 . Here, the functor L is as defined in Lemma 4.7, and thus $L(\{1\})$ and $L(\{1, 2\})$ represent the process networks $(\{1\}, \emptyset, \{\emptyset_{\bar{\mathbb{Z}}_2[\{1\}]}, \emptyset_{\bar{\mathbb{Z}}_2[\{1\}]}, \emptyset_{\bar{\mathbb{Z}}_2[\{1\}]}\})$ and $(\{1, 2\}, \emptyset, \{\emptyset_{\bar{\mathbb{Z}}_2[\{1,2\}]}, \emptyset_{\bar{\mathbb{Z}}_2[\{1,2\}]}, \emptyset_{\bar{\mathbb{Z}}_2[\{1,2\}]}\})$ respectively. The left interface \mathcal{I} specifies the entity e_{11}^b and the right interface \mathcal{O} specifies the entities e_{21}^b and e_{32}^b , through which the open process network interconnects with other open process networks.

Remark 4.10. To highlight the analogy of Definition 4.8 with an *open system*, a system that interacts with other systems, we call a process network with an interface also an open process

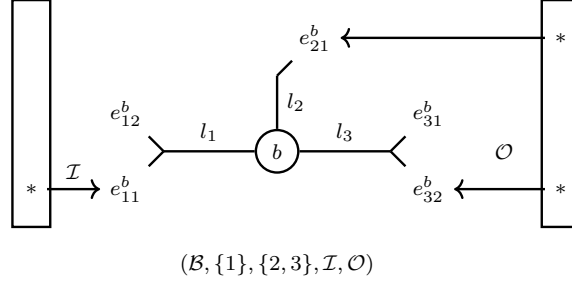


Figure 13: An illustration of an open process network discussed in Example 4.9.

network. These kinds of terminologies are common in Applied Category Theory literature; for example, in [7], authors have called Petri nets with interfaces as *open Petri nets*, in [8] and [33] respectively, authors called the reaction network with an interface and Markov process with an interface as an *open reaction network* and *open Markov process*.

Now, we need a technical lemma before we can construct our desired symmetric monoidal double category whose horizontal 1-morphisms are open process networks.

Lemma 4.11. For each $n \in \mathbb{N}$, the functor $L: \mathbf{Set} \rightarrow \mathbf{Process}_n$ has a right adjoint.

Proof. Let us define

$$\begin{aligned}
R: \mathbf{Process}_n &\rightarrow \mathbf{Set} \\
(E, B, \{l_i\}_n) &\rightarrow E \\
((\alpha, \beta): (E, B, \{l_i\}_n) \rightarrow (E', B', \{l'_i\}_n)) &\mapsto (\alpha: E \rightarrow E').
\end{aligned}$$

Observe that from the definition itself, it is clear that R is well-defined and is a functor. Now, we have the following natural isomorphisms:

$$\begin{aligned}
&\mathrm{hom}_{\mathbf{Bio}}(L(X), (E, B, \{l_i\}_n)) \\
&\cong \mathrm{hom}_{\mathbf{Bio}}\left((X, \emptyset, \underbrace{\{\emptyset_{\mathbb{Z}_2[X]}, \emptyset_{\mathbb{Z}_2[X]}, \emptyset_{\mathbb{Z}_2[X]}, \emptyset_{\mathbb{Z}_2[X]}\}}_{n\text{-times}}), (E, B, \{l_i\}_n)\right) \\
&\cong \mathrm{hom}_{\mathbf{Set}}(X, E) \text{ [As } \emptyset \text{ is an initial object in } \mathbf{Set}] \\
&\cong \mathrm{hom}_{\mathbf{Set}}\left(X, R((E, B, \{l_i\}_n))\right).
\end{aligned}$$

Hence, R is a left adjoint of L . □

We now have all the machinery to compose process networks with interfaces, as we see in our following result.

Theorem 4.12. Consider the functor $L: \mathbf{Set} \rightarrow \mathbf{Process}_n$ defined in Lemma 4.7. Then, there is a symmetric monoidal double category $\mathrm{Open}_{\mathrm{Double}}(\mathbf{Process}_n)$ whose

- objects are sets,
- vertical 1-morphisms are functions,
- horizontal 1-cells from a set X to a set Y are open process networks

$$\begin{array}{ccc}
& \mathcal{B} & \\
\mathcal{I} \nearrow & & \nwarrow \mathcal{O} \\
L(X) & & L(Y)
\end{array}$$

- A 2-morphism

$$\begin{array}{ccc}
& \mathcal{B} & \\
\mathcal{I} \nearrow & & \nwarrow \mathcal{O} \\
L(X) & & L(Y)
\end{array}
\Rightarrow
\begin{array}{ccc}
& \mathcal{B}' & \\
\mathcal{I}' \nearrow & & \nwarrow \mathcal{O}' \\
L(X') & & L(Y')
\end{array}$$

is given by a tuple $(f: X \rightarrow X', \eta: \mathcal{B} \rightarrow \mathcal{B}', g: Y \rightarrow Y')$, such that the following is a commutative diagram

$$\begin{array}{ccccc}
L(X) & \xrightarrow{\mathcal{I}} & \mathcal{B} & \xleftarrow{\mathcal{O}} & L(Y) \\
L(f) \downarrow & & \eta \downarrow & & \downarrow L(g) \\
L(X') & \xrightarrow{\mathcal{I}'} & \mathcal{B}' & \xleftarrow{\mathcal{O}'} & L(Y')
\end{array}$$

in $\mathbf{Process}_n$.

- Composition of 1-morphisms is the standard composition of functions.
- Composition of horizontal 1-cells is given by the composition of cospans via pushout constructions.

More precisely, suppose

$$\begin{array}{ccc}
& \mathcal{B} & \\
\mathcal{I}_1 \nearrow & & \nwarrow \mathcal{O}_1 \\
L(X) & & L(Y)
\end{array}
\quad \text{and} \quad
\begin{array}{ccc}
& \mathcal{A} & \\
\mathcal{I}_2 \nearrow & & \nwarrow \mathcal{O}_2 \\
L(Y) & & L(Z)
\end{array}$$

be two process networks. Then, the composite open process network is given by the following cospan from $L(X)$ to $L(Z)$ in $\mathbf{Process}_n$

$$\begin{array}{ccccc}
& & \mathcal{B} +_{L(Y)} \mathcal{A} & & \\
& & \nearrow & & \nwarrow \\
& \mathcal{B} & & & \mathcal{A} \\
\mathcal{I}_1 \nearrow & & \nwarrow \mathcal{O}_1 & & \nearrow \mathcal{I}_2 & \nwarrow \mathcal{O}_2 \\
L(X) & & L(Y) & & L(Z)
\end{array}$$

where $\mathcal{B} +_{L(Y)} \mathcal{A}$ is a chosen pushout square, and the unlabeled maps are the canonical maps to the pushout.

- the horizontal composition of 2-morphisms

$$\begin{array}{ccccc}
L(X) & \xrightarrow{\mathcal{I}_1} & \mathcal{B} & \xleftarrow{\mathcal{O}_1} & L(Y) \\
L(f) \downarrow & & \eta_1 \downarrow & & \downarrow L(g) \\
L(X') & \xrightarrow{\mathcal{I}'_1} & \mathcal{B}' & \xleftarrow{\mathcal{O}'_1} & L(Y')
\end{array}
\quad \text{and} \quad
\begin{array}{ccccc}
L(Y) & \xrightarrow{\mathcal{I}_2} & \mathcal{A} & \xleftarrow{\mathcal{O}_2} & L(Z) \\
L(g) \downarrow & & \eta_2 \downarrow & & \downarrow L(h) \\
L(Y') & \xrightarrow{\mathcal{I}'_2} & \mathcal{A}' & \xleftarrow{\mathcal{O}'_2} & L(Z')
\end{array}
\quad \text{is given as}$$

$$\begin{array}{ccccc}
L(X) & \longrightarrow & \mathcal{B} +_{L(Y)} \mathcal{A} & \longleftarrow & L(Z) \\
L(f) \downarrow & & \eta_2 +_{L(Y)} \eta_1 \downarrow & & \downarrow L(g) \\
L(X') & \longrightarrow & \mathcal{B}' +_{L(Y)} \mathcal{A}' & \longleftarrow & L(Z')
\end{array}$$

where the unlabeled maps are the canonical composite maps to the pushouts,

- vertical composition of 2-morphisms

$$\begin{array}{ccccc}
L(X) & \xrightarrow{\mathcal{I}} & \mathcal{B} & \xleftarrow{\mathcal{O}} & L(Y) \\
L(f) \downarrow & & \eta \downarrow & & \downarrow L(g) \\
L(X') & \xrightarrow{\mathcal{I}'} & \mathcal{B}' & \xleftarrow{\mathcal{O}'} & L(Y')
\end{array}$$

and

$$\begin{array}{ccccc} L(X') & \xrightarrow{\mathcal{I}'} & \mathcal{B}' & \xleftarrow{\mathcal{O}'} & L(Y') \\ L(f') \downarrow & & \eta' \downarrow & & \downarrow L(g') \\ L(X'') & \xrightarrow{\mathcal{I}''} & \mathcal{B}'' & \xleftarrow{\mathcal{O}''} & L(Y'') \end{array}$$

is defined using the composition of functions

$$\begin{array}{ccccc} L(X) & \xrightarrow{\mathcal{I}} & \mathcal{B} & \xleftarrow{\mathcal{O}} & L(Y) \\ L(f' \circ f) \downarrow & & \eta' \circ \eta \downarrow & & \downarrow L(g' \circ g) \\ L(X'') & \xrightarrow{\mathcal{I}''} & \mathcal{B}'' & \xleftarrow{\mathcal{O}''} & L(Y'') \end{array}$$

- The symmetric monoidal structure is derived from the coproducts in **Set** and **Process_n**. More precisely, the monoidal product is defined using chosen coproducts in **Set** and **Process_n**. Hence,

- the monoidal product of two finite sets X_1 and X_2 is the disjoint union $X_1 + X_2$,
- the monoidal product of two vertical 1-morphisms $f_1: X_1 \rightarrow Y_1$ and $f_2: X_2 \rightarrow Y_2$ is given by the natural map $f_1 + f_2: X_1 + X_2 \rightarrow Y_1 + Y_2$,
- the monoidal product of horizontal 1-cells

$$\begin{array}{ccccc} & & \mathcal{B}_1 & & \\ & \nearrow \mathcal{I}_1 & & \nwarrow \mathcal{O}_1 & \\ L(X_1) & & & & L(Y_1) \\ & & \text{and} & & \\ & & \mathcal{B}_2 & & \\ & \nearrow \mathcal{I}_2 & & \nwarrow \mathcal{O}_2 & \\ L(X_2) & & & & L(Y_2) \end{array} \quad \text{is given as}$$

$$\begin{array}{ccc} & \mathcal{B}_1 + \mathcal{B}_2 & \\ \nearrow \mathcal{I}_1 + \mathcal{I}_2 & & \nwarrow \mathcal{O}_1 + \mathcal{O}_2 \\ L(X_1 + X_2) & & L(Y_1 + Y_2) \end{array}$$

- the monoidal product of two 2-morphisms

$$\begin{array}{ccccc} L(X_1) & \xrightarrow{\mathcal{I}_1} & \mathcal{B}_1 & \xleftarrow{\mathcal{O}_1} & L(Y_1) \\ L(f_1) \downarrow & & \eta_1 \downarrow & & \downarrow L(g_1) \\ L(X'_1) & \xrightarrow{\mathcal{I}'_1} & \mathcal{B}'_1 & \xleftarrow{\mathcal{O}'_1} & L(Y'_1) \end{array} \quad \text{and} \quad \begin{array}{ccccc} L(X_2) & \xrightarrow{\mathcal{I}_2} & \mathcal{B}_2 & \xleftarrow{\mathcal{O}_2} & L(Y_2) \\ L(f_2) \downarrow & & \eta_2 \downarrow & & \downarrow L(g_2) \\ L(X'_2) & \xrightarrow{\mathcal{I}'_2} & \mathcal{B}'_2 & \xleftarrow{\mathcal{O}'_2} & L(Y'_2) \end{array} \quad \text{is given as}$$

$$\begin{array}{ccc} L(X_1 + X_2) & \xrightarrow{\mathcal{I}_1 + \mathcal{I}_2} & \mathcal{B}_1 + \mathcal{B}_2 & \xleftarrow{\mathcal{O}_1 + \mathcal{O}_2} & L(Y_1 + Y_2) \\ L(f_1 + f_2) \downarrow & & \eta_1 + \eta_2 \downarrow & & \downarrow L(g_1 + g_2) \\ L(X'_1 + X'_2) & \xrightarrow{\mathcal{I}'_1 + \mathcal{I}'_2} & \mathcal{B}'_1 + \mathcal{B}'_2 & \xleftarrow{\mathcal{O}'_1 + \mathcal{O}'_2} & L(Y'_1 + Y'_2) \end{array}$$

We consider initial objects as units for these monoidal products, and the symmetry is defined using the canonical isomorphism $X + Y \cong Y + X$.

Proof. Since the category **Process_n** is finitely cocomplete (Proposition 4.3), and the functor $L: \mathbf{Set} \rightarrow \mathbf{Process}_n$ has a right adjoint (Lemma 4.11), then the proof our theorem follows from the Lemma 14 of [7]. \square

The following two results respectively, show how the composition and the monoidal product of open process networks look explicitly in the light of Theorem 4.12.

Lemma 4.13. Consider two process networks $\mathcal{B}_1 = (E_1, B_1, \{l_{i_1}\}_n)$ and $\mathcal{B}_2 = (E_2, B_2, \{l_{i_2}\}_n)$ in **Process_n**. Let $\mathcal{O}_1: L(Y) \rightarrow \mathcal{B}_1$ and $\mathcal{I}_2: L(Y) \rightarrow \mathcal{B}_2$ be two morphisms in the category **Process_n**, where $L: \mathbf{Set} \rightarrow \mathbf{Process}_n$ is the functor as defined in Lemma 4.7. Then, the pushout biochemical process network $\mathcal{B}_1 +_{\mathcal{O}_1, L(Y), \mathcal{I}_2} \mathcal{B}_2 = (E, B, \{l_i\}_n)$ exists, and the following defines a pushout upto an isomorphism:

- $E := E_1 +_{\mathcal{O}_1, Y, \mathcal{I}_2} E_2$, where $\mathcal{O}_1: Y \rightarrow E_1$ and $\mathcal{I}_2: Y \rightarrow E_2$ are the underlying canonical functions associated to \mathcal{O}_1 and \mathcal{I}_2 , respectively.
- $B := B_1 \sqcup B_2$.
- For each $i \in \{1, 2, \dots, n\}$, $l_i: B \rightarrow \bar{\mathbb{Z}}_2[E]$ is defined as

$$\begin{aligned} l_i: B &\rightarrow \bar{\mathbb{Z}}_2[E] \\ (b_1, B_1) &\mapsto \bar{\mathbb{Z}}_2[j_1](l_{i_1}(b_1)) \\ (b_2, B_2) &\mapsto \bar{\mathbb{Z}}_2[j_2](l_{i_2}(b_2)), \end{aligned}$$

where $j_1: E_1 \rightarrow E, x \mapsto [(x, E_1)]$ and $j_2: E_2 \rightarrow E, x \mapsto [(x, E_2)]$, where $[\]$ represents the equivalence class.

Proof. The existence of pushout is a direct consequence of Theorem 4.3. Checking $\mathcal{B}_1 +_{\mathcal{O}_1, L(Y), \mathcal{I}_2} \mathcal{B}_2$ is indeed a pushout in **Process_n** is a routine verification. \square

Lemma 4.14. Consider two process networks $\mathcal{B}_1 = (E_1, B_1, \{l_{i_1}\}_n)$ and $\mathcal{B}_2 = (E_2, B_2, \{l_{i_2}\}_n)$ in **Process_n**. Then, the coproduct biochemical process network $\mathcal{B}_1 + \mathcal{B}_2 = (E, B, \{l_i\}_n)$ exists in **Process_n**, and the following defines a coproduct upto an isomorphism:

- $E := E_1 \sqcup E_2$.
- $B := B_1 \sqcup B_2$.
- For each $i \in \{1, 2, \dots, n\}$, $l_i: B \rightarrow \bar{\mathbb{Z}}_2[E]$ is defined as

$$\begin{aligned} l_i: B &\rightarrow \bar{\mathbb{Z}}_2[E] \\ (b_1, B_1) &\mapsto \bar{\mathbb{Z}}_2[j_1](l_{i_1}(b_1)) \\ (b_2, B_2) &\mapsto \bar{\mathbb{Z}}_2[j_2](l_{i_2}(b_2)), \end{aligned}$$

where $j_1: E_1 \rightarrow E, x \mapsto (x, E_1)$ and $j_2: E_2 \rightarrow E, x \mapsto (x, E_2)$.

Proof. Follows directly from Lemma 4.13. \square

Example 4.15 (Combining open process networks using the composition laws of horizontal 1-morphisms). In Figure 14, we illustrate the composition of open process networks $(\mathcal{B}, \{1\}, \{2, 3\}, \mathcal{I}, \mathcal{O})$ and $(\mathcal{B}', \{2, 3\}, \{4\}, \mathcal{I}', \mathcal{O}')$, where

$$\mathcal{B} = (\{e_{11}^b, e_{12}^b, e_{21}^b, e_{31}^b, e_{32}^b\}, \{b\}, \{l_i\}_3)$$

and

$$\mathcal{B}' = (\{e_{11}^{b'}, e_{12}^{b'}, e_{31}^{b'}, e_{32}^{b'}\}, \{b'\}, \{l'_i\}_3)$$

are process networks. Here, the functor L is as defined in Lemma 4.7. While composing using Theorem 4.12, the right interface \mathcal{O} of $(\mathcal{B}, \{1\}, \{2, 3\}, \mathcal{I}, \mathcal{O})$ and the left interface \mathcal{I}' of $(\mathcal{B}', \{2, 3\}, \{4\}, \mathcal{I}', \mathcal{O}')$ specify the entities to be identified. In particular, they identify e_{21}^b and $e_{12}^{b'}$ as an entity e and identify e_{32}^b and $e_{11}^{b'}$ as an entity d . The process network $\mathcal{B} +_{\mathcal{O}, L(\{2,3\}), \mathcal{I}'} \mathcal{B}'$ in the composite open process network $(\mathcal{B} +_{\mathcal{O}, L(\{2,3\}), \mathcal{I}'} \mathcal{B}', \{1\}, \{4\}, \mathcal{I}, \mathcal{O}', \mathcal{B}')$ is computed using the specification given in Lemma 4.13. Explicitly, $\mathcal{B} +_{\mathcal{O}, L(\{2,3\}), \mathcal{I}'} \mathcal{B}' = (\{e_{11}^b, e_{12}^b, e, e_{31}^b, d, e_{31}^{b'}, e_{32}^{b'}\}, \{b, b'\}, \{\bar{l}_i\}_3)$, where the functions \bar{l}_i are evident in the Figure 14.

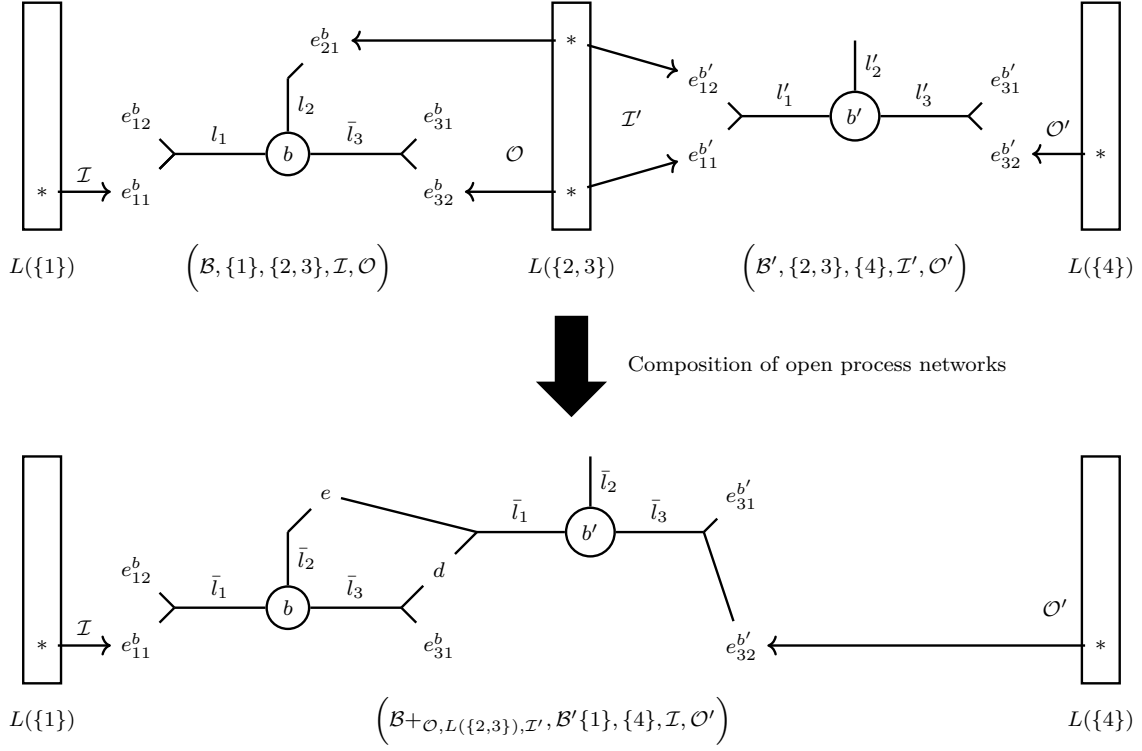


Figure 14: An illustration of composing open process networks using the composition law of horizontal 1-morphisms in Theorem 4.12, see Example 4.15.

Example 4.16 (Combining open process networks using the monoidal product of horizontal 1-morphisms). In Figure 15, we illustrate the monoidal product of open process networks $(\mathcal{B}, \{1\}, \{4\}, \mathcal{I}, \mathcal{O})$ and $(\mathcal{B}', \{2, 3\}, \{5\}, \mathcal{I}', \mathcal{O}')$ using the monoidal product defined in Theorem 4.12, where $\mathcal{B} = (\{e_{11}^b, e_{12}^b, e_{21}^b, e_{31}^b, e_{32}^b\}, \{b\}, \{\bar{l}_i\}_3)$ and $\mathcal{B}' = (\{e_{11}^{b'}, e_{12}^{b'}, e_{31}^{b'}, e_{32}^{b'}\}, \{b'\}, \{\bar{l}'_i\}_3)$. Here, the functor L is as defined in Lemma 4.7. Observe that the process network $\mathcal{B} + \mathcal{B}'$ in the composite open process network $(\mathcal{B} + \mathcal{B}', \{1\} \sqcup \{2, 3\}, \{4\} \sqcup \{5\}, \mathcal{I} + \mathcal{I}', \mathcal{O} + \mathcal{O}')$ is computed using the specification given in Lemma 4.14. Explicitly, the process network

$$\mathcal{B} + \mathcal{B}' = (\{e_{11}^b, e_{12}^b, e_{21}^b, e_{31}^b, e_{32}^b, e_{11}^{b'}, e_{12}^{b'}, e_{31}^{b'}, e_{32}^{b'}\}, \{b, b'\}, \{\bar{l}_i\}_3),$$

where the functions \bar{l}_i are evident in the Figure 15.

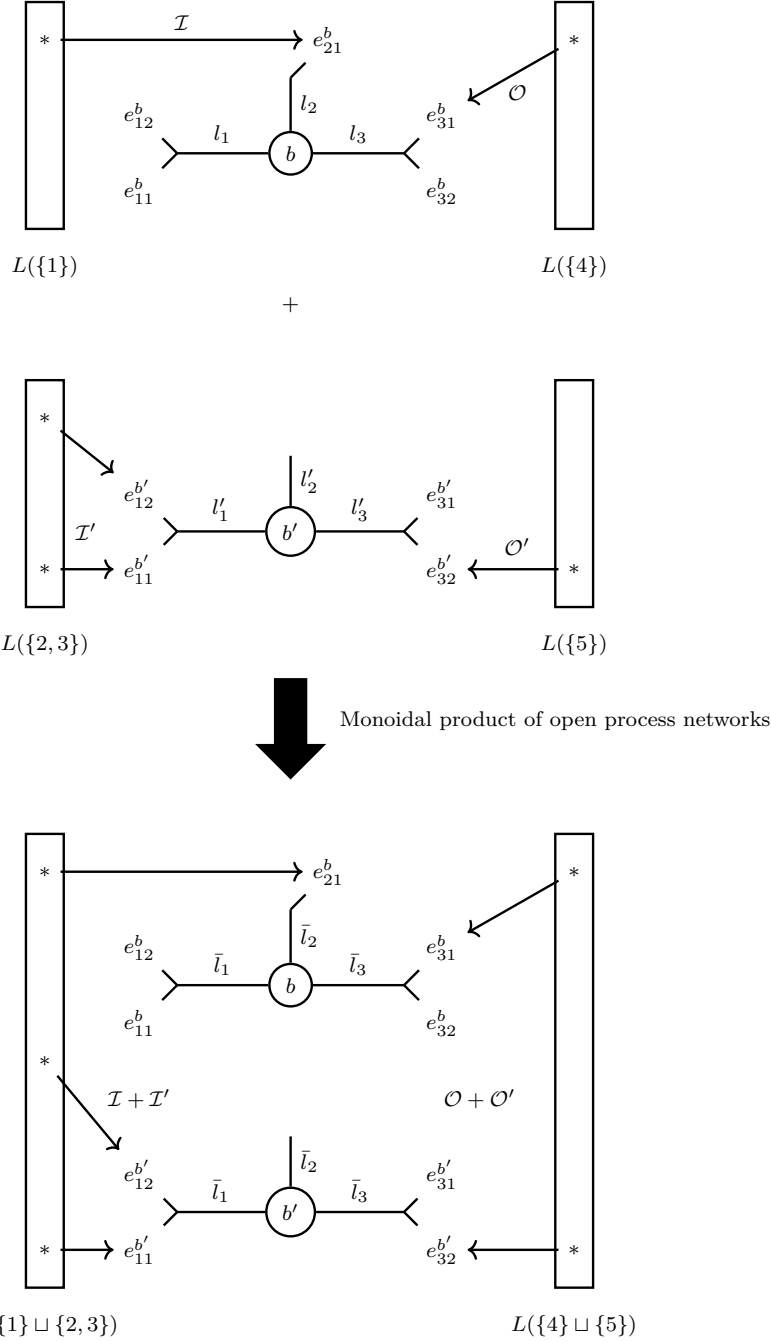


Figure 15: An illustration of combining open process networks using the monoidal product defined in Theorem 4.12, see Example 4.16. We combine the open process networks $(\mathcal{B}, \{1\}, \{4\}, \mathcal{I}, \mathcal{O})$ (top) and $(\mathcal{B}', \{2, 3\}, \{5\}, \mathcal{I}', \mathcal{O}')$ (top) to obtain the open process network $(\mathcal{B} + \mathcal{B}', \{1\} \sqcup \{2, 3\}, \{4\} \sqcup \{5\}, \mathcal{I} + \mathcal{I}', \mathcal{O} + \mathcal{O}')$ (below).

Example 4.17 (2-morphism between two open process networks). In Figure 16, we illustrate a 2-morphism $(\text{id}_{\{1\}}: \{1\} \rightarrow \{1\}, \eta: \mathcal{B} \rightarrow \mathcal{B}', \text{id}_{\{2,3\}}: \{2, 3\} \rightarrow \{2, 3\})$ from the open process network $(\mathcal{B}, \{1\}, \{2, 3\}, \mathcal{I}, \mathcal{O})$ to the open process network $(\mathcal{B}', \{1\}, \{2, 3\}, \mathcal{I}', \mathcal{O}')$, where $\mathcal{B} = (E = \{e_{11}^b, e_{12}^b, e_{21}^b, e_{31}^b, e_{32}^b\}, B = \{b\}, \{l_i\}_3)$ and $\mathcal{B}' = (E' = \{e_{11}^b, e_{21}^b, e_{31}^b\}, B' = \{b\}, \{l'_i\}_3)$ are process networks. Here, $\eta := (\alpha: E \rightarrow E', \beta: B \rightarrow B')$ is a morphism of process networks, where β is the identity map on the set $\{b\}$, and α maps $e_{11}^b \mapsto e_{11}^b, e_{12}^b \mapsto e_{11}^b, e_{21}^b \mapsto e_{21}^b, e_{31}^b \mapsto e_{32}^b, e_{32}^b \mapsto e_{32}^b$, and hence we have $\mathcal{I}' \circ L(\text{id}_{\{1\}}) = \eta \circ \mathcal{I}$ and $\mathcal{O}' \circ L(\text{id}_{\{2,3\}}) = \eta \circ \mathcal{O}$.

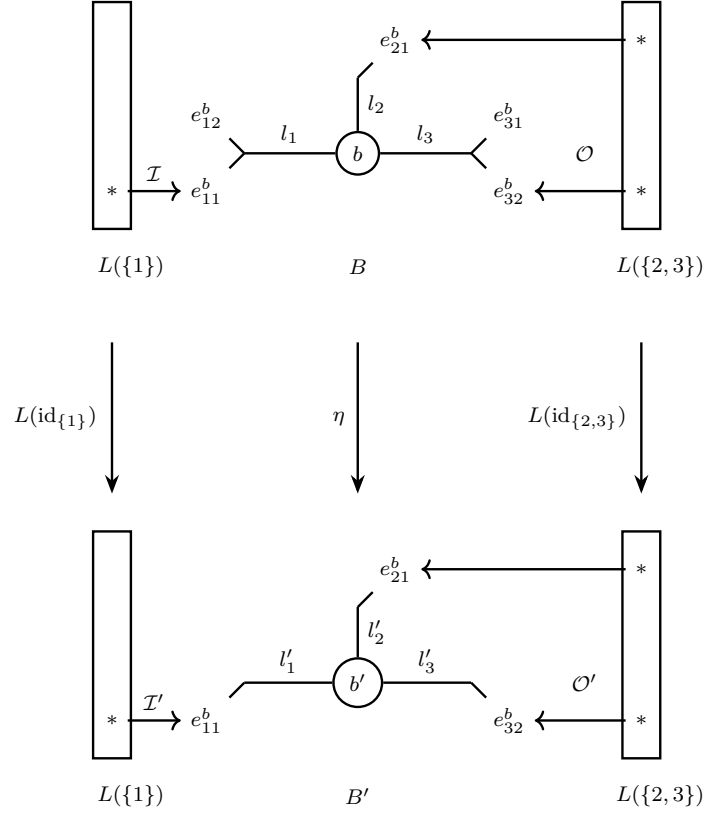


Figure 16: An illustration of 2-morphism between two open process networks, see Example 4.17.

Example 4.18 (Horizontal composition of 2-morphisms). In Figure 17 and Figure 18, we illustrate the horizontal composition of the 2-morphism $(\text{id}_{\{2,3\}}, \eta_2, \text{id}_{\{4\}})$ from the open process network $(\mathcal{B}_2, \{2, 3\}, \{4\}, \mathcal{I}_2, \mathcal{O}_2)$ to the open process network $(\mathcal{B}'_2, \{2, 3\}, \{4\}, \mathcal{I}'_2, \mathcal{O}'_2)$, and the 2-morphism $(\text{id}_{\{1\}}, \eta_1, \text{id}_{\{2,3\}})$ from the open process network $(\mathcal{B}_1, \{1\}, \{2, 3\}, \mathcal{I}_1, \mathcal{O}_1)$ to the open process network $(\mathcal{B}'_1, \{1\}, \{2, 3\}, \mathcal{I}'_1, \mathcal{O}'_1)$. 2-morphisms η_2 and η_1 are shown in Figure 17, and their horizontal composition $\eta_2 +_{L(\text{id}_{\{2,3\}})} \eta_1$ is shown in Figure 18. Note that here the horizontal composition of open process networks identifies the entities $e_{21}^{b_1}$ and $e_{21}^{b_2}$ into the entity e , and identifies the entities $e_{31}^{b_1}$ and $e_{11}^{b_2}$ into d .

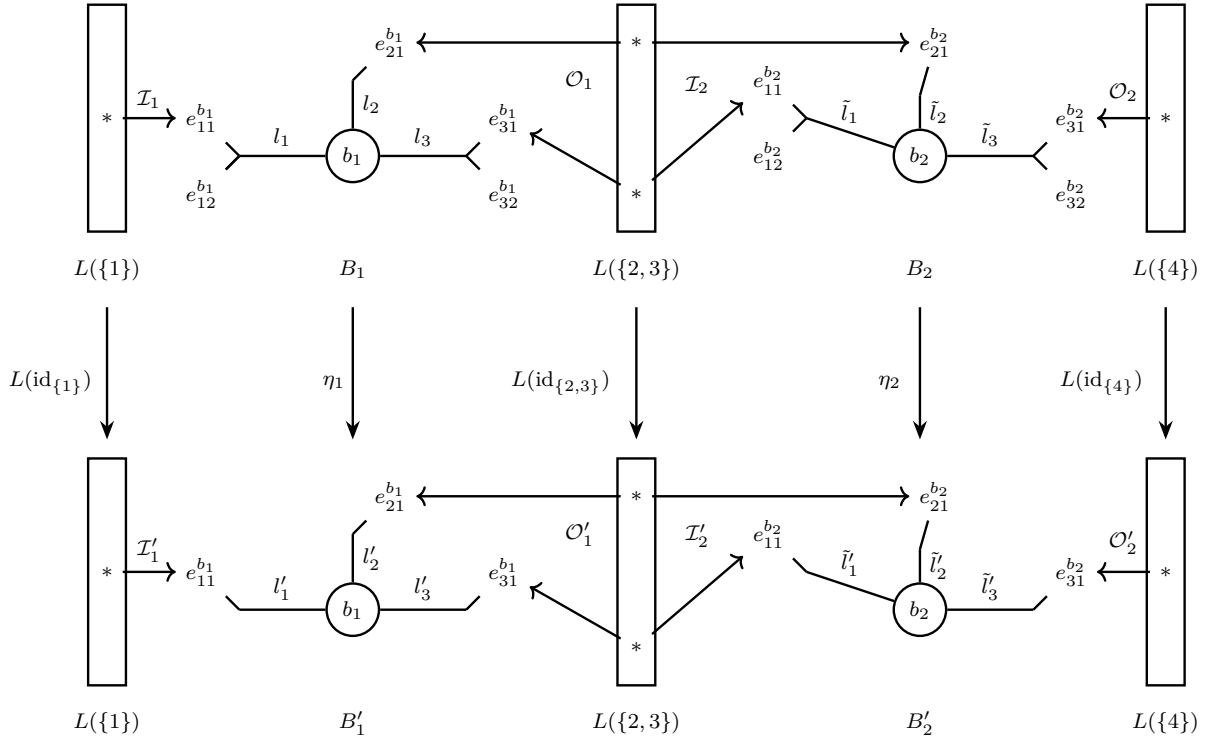


Figure 17: An illustration showing 2-morphisms between composable horizontal 1-morphisms considered in Example 4.18.

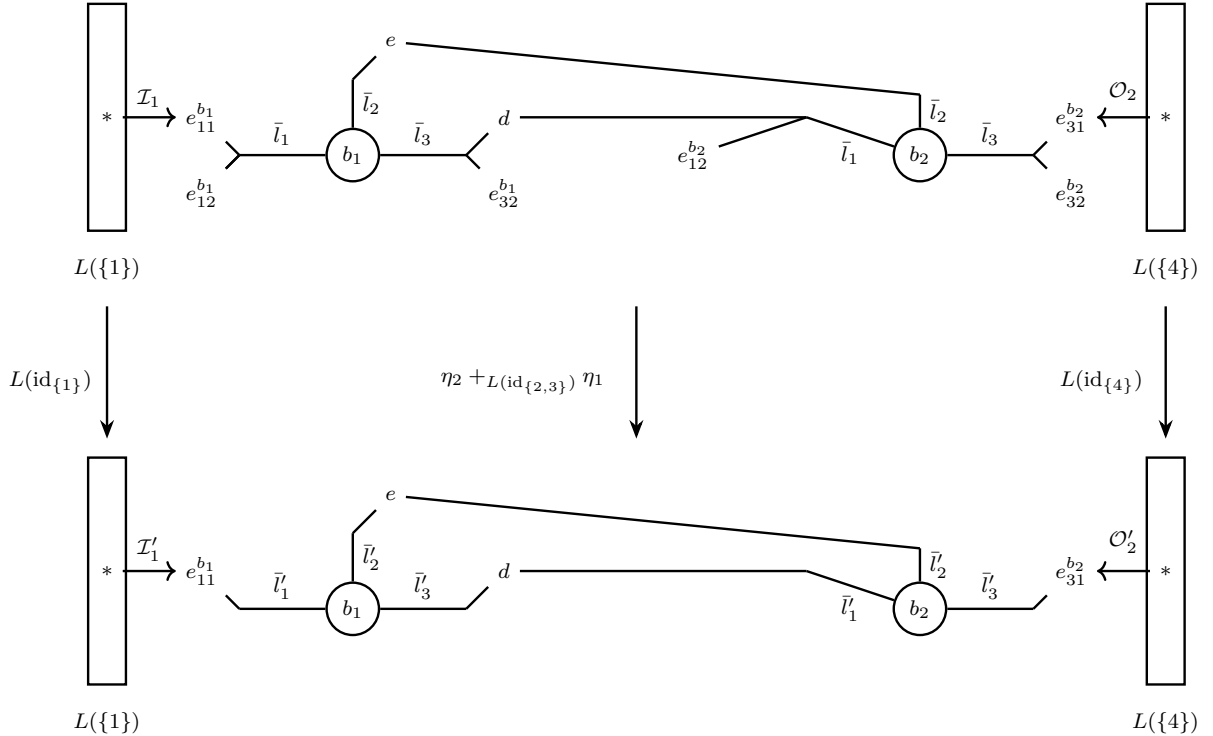


Figure 18: An illustration of horizontal composition of the 2-morphisms as shown in Example 4.18.

Example 4.19 (Compatibility between compositionality and zooming-out process). Using SBGN-PD visualisations, in Figure 19, we demonstrate how the horizontal composition law of 2-morphisms

as in Theorem 4.12 (see Example 4.18) induces a compatibility condition between compositionality and zooming-out process in a system of biochemical reaction networks. In particular, we start with two biochemical reactions numbered (1) and (2). Then, using the 2-morphisms as shown in Figure 17, we zoom-out (shown with the thin black arrows) by forgetting ADP's and ATP's from the reactions, and we obtain the biochemical reactions (3) from (1), and (4) from (2). Then, using the horizontal composition of 1-morphisms (shown with dotted black lines) as in Figure 18, we combine (3) and (4) to obtain the reaction network (6), and the reactions (1) and (2) to get reaction network (5). The horizontal composition of two 2-morphisms (as in Figure 18) provides us with a canonical way of combining two zooming-out procedures ((1) to (3) and (2) to (4)) such that the combined zoom-out procedure behaves well with the composition of process networks. To be more precise, the combined zoom-out process takes the reaction network (5) to the reaction network (6).

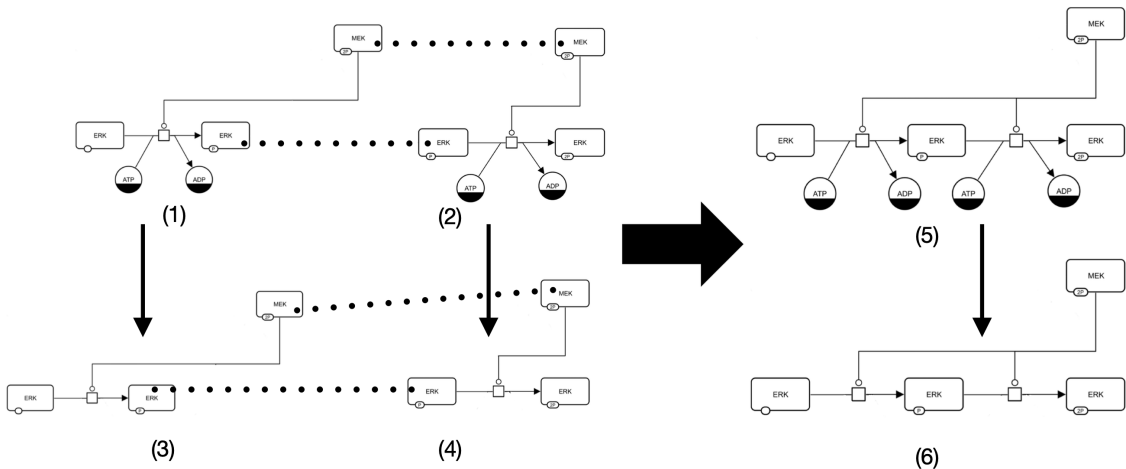


Figure 19: An illustration of a compatibility condition between compositionality and zooming-out process in a system of biochemical reaction networks visualised in SBGN-PD (see Example 4.19). SBGN images are derived from the MAPK cascade example on Page 65, [35].

In the Example 4.18, we explained how one can interpret the horizontal composition of 2-morphisms as a compatibility condition between the zooming-out procedures and composition laws of process networks. In the same spirit, one can interpret the monoidal product of 2-morphisms as a compatibility condition between the zooming-out procedures and the monoidal product of process networks.

4.3 Macroscopic of a process network

This subsection builds a mathematical gadget by the name *macroscope*, which provides us with a formal language to describe the influence of a particular portion of a biochemical network on the remaining portion and vice versa. To achieve our said purpose, we introduce a few technical notions below.

Definition 4.20 (Process subnetwork of a process network). A *process subnetwork* of a process network $\mathcal{B} = (E, B, \{l_i\}_n)$ is a process network $\mathcal{B}' = (E', B', \{l'_i\}_n)$ such that $E' \subseteq E$ and $B' \subseteq B$ and $l'_i(b) = l_i(b)$ for all $b \in B'$ and $i \in \{1, 2, \dots, n\}$.

Definition 4.21 (Environment of a process subnetwork). Let $\mathcal{B}' = (E', B', \{l'_i\}_n)$ be a process subnetwork of a process network $\mathcal{B} = (E, B, \{l_i\}_n)$. Then the *environment* of \mathcal{B}' with respect to \mathcal{B} is defined as the subset $B - B'$.

Definition 4.22. Let $\mathcal{B}' = (E', B', \{l'_i\}_n)$ be a process subnetwork of a process network $\mathcal{B} = (E, B, \{l_i\}_n)$. Then for each $i \in \{1, 2, \dots, n-1\}$, using the notations as in the Remark 3.3, we define the $M_i^{\mathcal{B}, \mathcal{B}'}$ -function of \mathcal{B}' as follows:

$$\begin{aligned} M_i^{\mathcal{B}, \mathcal{B}'} : E' &\rightarrow \bar{\mathbb{Z}}_2[E'] \\ e &\mapsto e, \text{ if there exists } b \in B - B' \text{ and } b' \in B' \text{ such that } e = e_{nj}^b = e_{ij'}^{b'} \\ &\quad \text{for some } j \in \{1, 2, \dots, m_b^n\} \text{ and } j' \in \{1, 2, \dots, m_{b'}^i\}, \\ e &\mapsto 0, \text{ otherwise.} \end{aligned}$$

and, when $i = n$, we have

$$\begin{aligned} M_n^{\mathcal{B}, \mathcal{B}'} : E' &\rightarrow \bar{\mathbb{Z}}_2[E'] \\ e &\mapsto e, \text{ if there exists } b \in B - B' \text{ and } b' \in B' \text{ such that } e = e_{kj}^b = e_{nj'}^{b'}, \\ &\quad \text{for some } k \in \{1, 2, \dots, n-1\}, j \in \{1, 2, \dots, m_b^k\}, j' \in \{1, 2, \dots, m_{b'}^n\}, \\ e &\mapsto 0, \text{ otherwise.} \end{aligned}$$

Given a process network $\mathcal{B} = (E, B, \{l_i\}_n)$, for each $i \in \{1, 2, \dots, n-1, n\}$, one can extend the function $M_i^{\mathcal{B}, \mathcal{B}'} : E' \rightarrow \bar{\mathbb{Z}}_2[E']$ to a function

$$\begin{aligned} \overline{M_i^{\mathcal{B}, \mathcal{B}'}} : \bar{\mathbb{Z}}_2[E'] &\rightarrow \bar{\mathbb{Z}}_2[E'] \\ (\alpha_1 e_1 + \alpha_2 e_2 + \dots + \alpha_n e_n) &\mapsto (\alpha_1 M_i^{\mathcal{B}, \mathcal{B}'}(e_1) + \alpha_2 M_i^{\mathcal{B}, \mathcal{B}'}(e_2) + \dots + \alpha_n M_i^{\mathcal{B}, \mathcal{B}'}(e_n)). \end{aligned}$$

We need to make one more technical definition before introducing our intended *macroscope*.

Definition 4.23. Given a process network $\mathcal{B} = (E, B, \{l_i\}_n)$, we define the $\Sigma_{\mathcal{B}}$ -function of the process network \mathcal{B} as follows:

$$\begin{aligned} \Sigma_{\mathcal{B}} : \mathcal{L} &\rightarrow \bar{\mathbb{Z}}_2[E] \\ l_i &\mapsto \sum_{b \in B} (l_i(b)), \text{ for each } i \in \{1, 2, \dots, n\}, \end{aligned}$$

where \mathcal{L} is the set $\{l_1, l_2, \dots, l_n\}$.

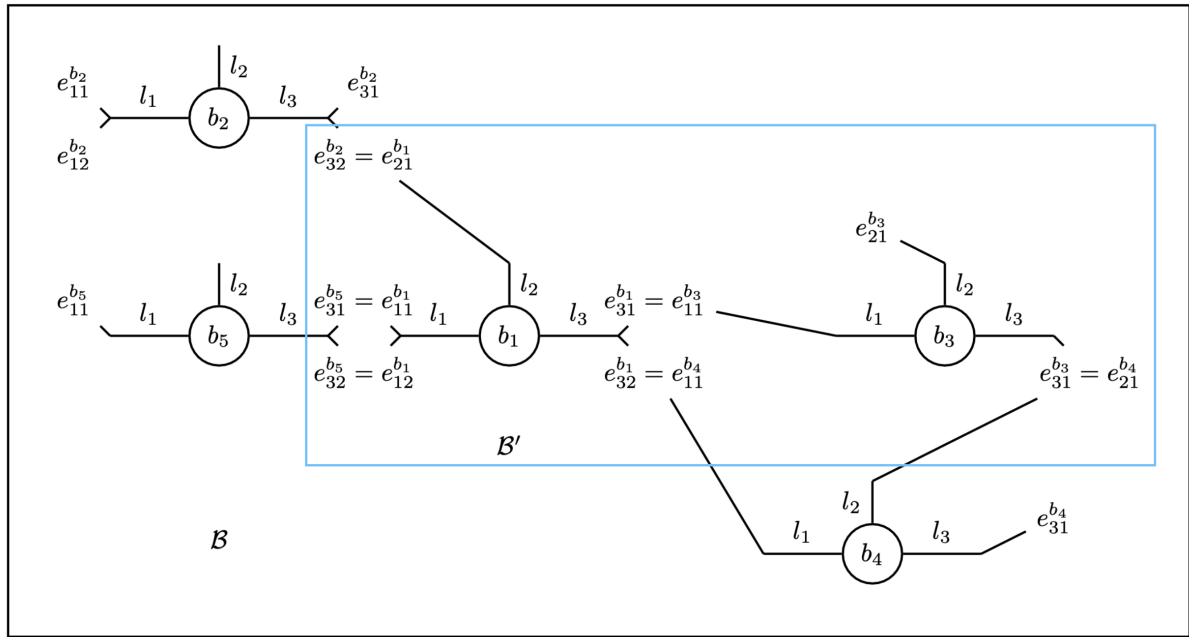
Definition 4.24 (Macroscope of a process subnetwork). Let $\mathcal{B}' = (E', B', \{l'_i\}_n)$ be a process subnetwork of a process network $\mathcal{B} = (E, B, \{l_i\}_n)$. Then, the *macroscope of \mathcal{B}' with respect to \mathcal{B}* is defined as the n -tuple $M(\mathcal{B}, \mathcal{B}') := (L_1^{\mathcal{B}, \mathcal{B}'}, L_2^{\mathcal{B}, \mathcal{B}'}, \dots, L_n^{\mathcal{B}, \mathcal{B}'}) \in \bar{\mathbb{Z}}_2[E'] \times \bar{\mathbb{Z}}_2[E'] \times \dots \times \bar{\mathbb{Z}}_2[E']$, where

$$L_i^{\mathcal{B}, \mathcal{B}'} := \overline{M_i^{\mathcal{B}, \mathcal{B}'}}(\Sigma_{\mathcal{B}'}(l_i)), \quad \forall i \in \{1, 2, \dots, n\}.$$

For each $i \in \{1, 2, \dots, n-1\}$, the i -th coordinate $L_i^{\mathcal{B}, \mathcal{B}'}$ is called the l_i -influence of the environment on \mathcal{B}' , and the n -th coordinate $L_n^{\mathcal{B}, \mathcal{B}'}$ is called the influence of \mathcal{B}' on its environment.

Remark 4.25. Using the notations as in Definition 4.24, note that when $\mathcal{B} = \mathcal{B}'$, we have $M(\mathcal{B}, \mathcal{B}') = \underbrace{(0, 0, \dots, 0)}_{n\text{-times}}$.

Example 4.26. In Figure 20, we illustrate a process subnetwork \mathcal{B}' (marked with a blue rectangle) of a process network \mathcal{B} (marked with a black rectangle) with three legs. Note that the environment of \mathcal{B}' with respect to \mathcal{B} is the set $\{b_1, b_2, b_3, b_4, b_5\} - \{b_1, b_3\} = \{b_2, b_4, b_5\}$. Observe that $M(\mathcal{B}, \mathcal{B}') = (e_{11}^{b_1} + e_{12}^{b_1}, e_{21}^{b_1}, e_{32}^{b_1} + e_{31}^{b_3})$. The first coordinate $e_{11}^{b_1} + e_{12}^{b_1}$ and the second coordinate $e_{21}^{b_1}$ of $M(\mathcal{B}, \mathcal{B}')$ describes the l_1 -influence and l_2 -influence of the environment on \mathcal{B}' , respectively, and the 3rd coordinate $e_{32}^{b_1} + e_{31}^{b_3}$ describes the influence of \mathcal{B}' on its environment.



Applying macroscope of \mathcal{B}' with respect to \mathcal{B}

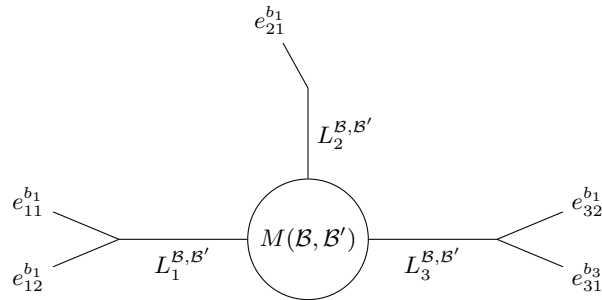
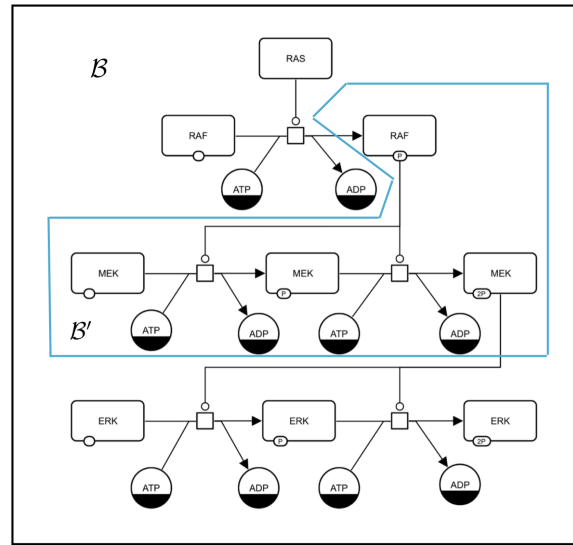


Figure 20: Visualisation of the macroscope discussed in Example 4.26.

Example 4.27. In Figure 21, we illustrate Definition 4.24 on the SBGN-PD visualisation of the MAPK cascade. Here, we mark \mathcal{B}' with blue and \mathcal{B} with black. The macroscope $M(\mathcal{B}, \mathcal{B}')$ of \mathcal{B}' with respect to \mathcal{B} is $(0, (\text{RAF-P}, \text{macromolecule}), (\text{MEK-2P}, \text{macromolecule}))$. Notations MEK-2P and RAF-P describe a double phosphorylated MEK and phosphorylated RAF, respectively. In the representation of the form (a, b) , the first coordinate a represents the molecule, and the second coordinate b represents its type. It says that the biochemical reaction network marked in red modulates its environment via $(\text{MEK-2P}, \text{macromolecule})$; on the other hand, the environment modulates it via $(\text{RAF-P}, \text{macromolecule})$.



Applying macroscope of \mathcal{B}' with respect to \mathcal{B}

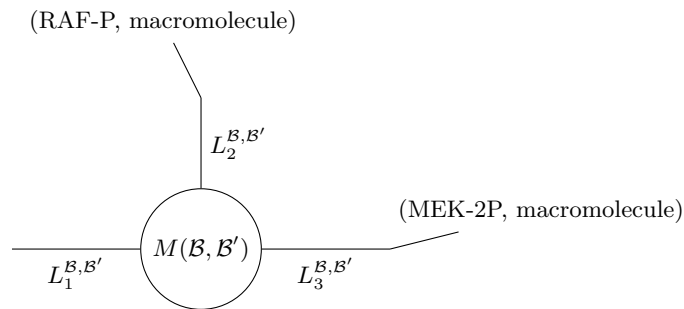


Figure 21: Visualisation of a macroscope (Definition 4.24) on the SBGN-PD visualisation of the MAPK cascade as discussed in Example 4.27. The SBGN image is taken from the MAPK cascade example on Page 65 in [35].

5 Translation of SBGN-PD into process networks

Although in Section 3 and Section 4, we have illustrated our theory of process networks using SBGN-PD visualisations, we have not explicitly discussed the methodologies of translating SBGN visualisations into process networks (Definition 3.1). This section attempts to fill this gap by developing formal methods to translate SBGN-PD visualisations of biochemical networks into our process networks. As a consequence, we would have the mathematical theory developed in Section 3 and Section 4 at our disposal, to apply on any SBGN-PD visualisation. This would provide us with an organisational principle for any molecular/cellular network visualised using SBGN-PD. However, since SBGN visualisations are by itself not a mathematical model, our treatment in this section is subject to further improvements in future.

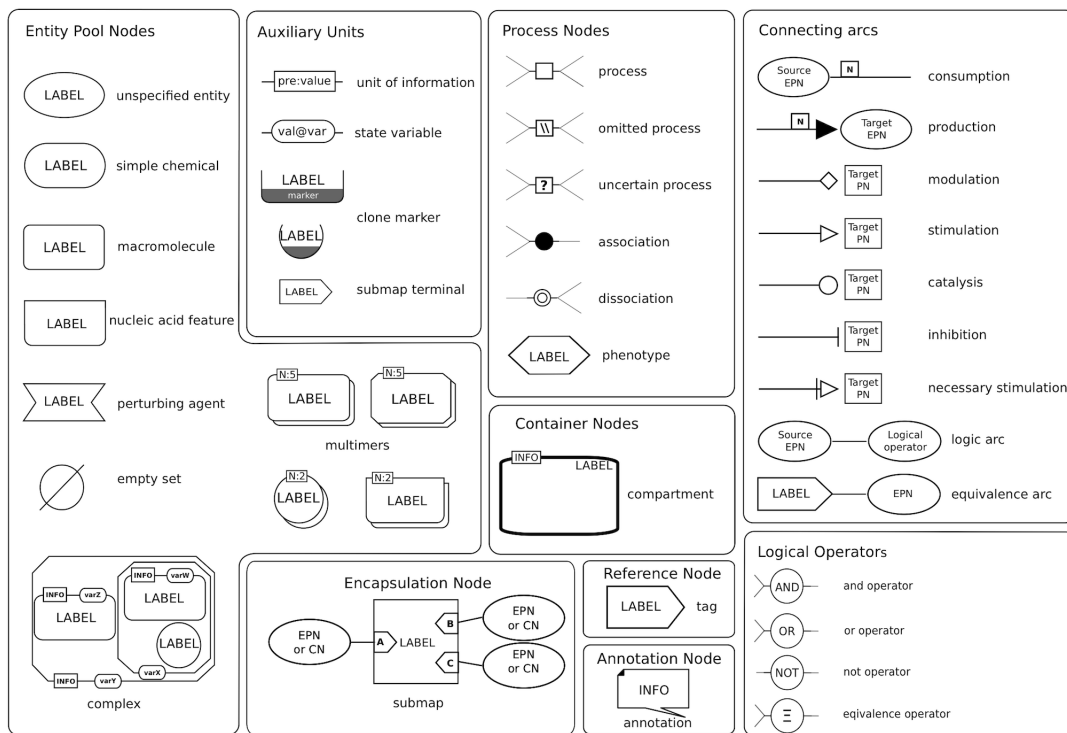


Figure 22: Reference card for SBGN PD language Level 1 Version 2.0. The image is taken from Page 75, [35].

5.1 When a SBGN-PD has no logical operators, encapsulation nodes, reference nodes, logic arcs and equivalence arcs

5.1.1 Entity pool nodes (as in Figure 22) to entities (as in Definition 3.1)

An SBGN-PD visualisation of a molecular/cellular network carries various information about the entity pool nodes involved in the network representation. For example, through *compartment nodes*, it describes the location of an entity pool node and distinguishes between identical biochemical entities located in different compartments. Using various geometric shapes like rectangles with rounded corners, circles, etc., to represent entity pool nodes, an SBGN-PD visualisation tells the ‘type’ (like macromolecule, simple chemical, etc.) of the entity pool nodes used in the network. Furthermore, such nodes may contain additional pieces of information like state variables, units of information etc. Given a SBGN-PD say Γ , to capture this information within the formal framework of a process network (Definition 3.1), we first enumerate the compartments involved in Γ , say $C_1, C_2, \dots, C_m, m \in \mathbb{N}$. Now, for each $i \in \{1, 2, \dots, m\}$, we define X_i as the set containing ‘meaningful words and symbols’ (w.r.t SBGN-PD, level 1, version 2.0, terminologies [35]) on each entity pool node used and located in the compartment C_i of Γ . If multiple words/symbols are used, we write the words/symbols in any permutation but separated by ‘-’. Then we consider the set \mathcal{T} which contains the ‘types’ of the entity pool nodes used in Γ . For example, an element of \mathcal{T} can be the words "macromolecule", "simple chemical", "complex", "multimer" etc. Then, we define a set $\mathcal{E}_\Gamma := (\sqcup_{i \in \{1, 2, \dots, m\}} X_i) \times \mathcal{T}$, where \sqcup is the disjoint union of sets. Let us illustrate how the elements of \mathcal{E}_Γ looks if we take Γ as the SBGN-PD visualisation of the IGF signalling (Figure 5). Here, $m = 2$, where without loss of a generality, we can take C_1 is EXTRACELLULAR and C_2 is CYTOSOL. Here, $\mathcal{T} = \{ \text{macromolecule, simple chemical, complex} \}$. For example, consider the macromolecule double-phosphorylated ERK located in C_2 . Then, as an element of \mathcal{E}_Γ , it has the

following equivalent descriptions viz.

$$\left(\left(\underbrace{\text{ERK-2P}}_{\text{meaningful words and symbols}}, C_2 \right), \text{macromolecule} \right)$$

or

$$\left(\left(\underbrace{\text{2P-ERK}}_{\text{meaningful words and symbols}}, C_2 \right), \text{macromolecule} \right).$$

Now, consider the complex in C_2 which is formed from the association of the macromolecule SOS and the macromolecule Grb2. As an element in \mathcal{E}_Γ , it is equivalently described as

$$\left(\left(\underbrace{\left(\left(\text{SOS}, C_2 \right), \text{macromolecule} \right) - \left(\left(\text{Grb2}, C_2 \right), \text{macromolecule} \right)}_{\text{meaningful words and symbols}}, C_2 \right), \text{complex} \right)$$

or

$$\left(\left(\underbrace{\left(\left(\text{Grb2}, C_2 \right), \text{macromolecule} \right) - \left(\left(\text{SOS}, C_2 \right), \text{macromolecule} \right)}_{\text{meaningful words and symbols}}, C_2 \right), \text{complex} \right).$$

We will later see that the elements of \mathcal{E}_Γ would be the entities (as in Definition 3.1) in the associated process network \mathcal{B}_Γ .

5.1.2 From process nodes (as in Figure 22) to process species (as in Definition 3.1)

In a SBGN-PD, various *process nodes* (see Figure 22) are used to denote biological processes and are distinguished using different geometric shapes according to the roles they are playing. For example, a small white square for a usual biochemical reaction, a small black circle to denote association etc. Let Γ be an SBGN-PD, and without loss of any generality, we label all the process nodes in Γ (assuming the set of process nodes in Γ is finite). A unique label is assigned to each process node. Let the set of all labels on the process nodes of Γ be denoted as B_Γ . We will later see that the elements of \mathcal{B}_Γ would be the process species (as in Definition 3.1) in the associated process network \mathcal{B}_Γ .

5.1.3 From connecting arcs (as in Figure 22) to legs (as in Definition 3.1)

Various *connecting arcs* (between process nodes and entity pool nodes) are used in an SBGN-PD. They are characterised according to the ‘context’ in which they are associated to the connected process nodes, and are distinguished by different geometric shapes. For example, in an SBGN-PD, different geometric shapes are used to denote consumption arc, production arc, stimulation arc, inhibition arc, etc (see Figure 22). Let Γ be an SBGN-PD and A_Γ be the set containing the ‘types’ of connecting arcs used in Γ , and we label the elements of the set A_Γ as a_1, a_2, \dots, a_k , preferably the production arc (if present) as a_k . Using the notations from 5.1.1, assuming $\mathcal{E}_\Gamma = (\sqcup_{i \in \{1, 2, \dots, m\}} X_i) \times \mathcal{T}$ as finite, we label the elements of \mathcal{E}_Γ as e_1, e_2, \dots, e_r , for $r \in \mathbb{N}$ without loss of any generality. Using the notation from 5.1.2, for each $i \in \{1, 2, \dots, n\}$, we define function $l_i^\Gamma : B_\Gamma \rightarrow \overline{\mathbb{Z}}_2[\mathcal{E}_\Gamma]$ that takes a process node/process species $b \in B_\Gamma$ to a formal linear combination $\alpha_1 e_1 + \alpha_2 e_2 + \dots + \alpha_r e_r \in \overline{\mathbb{Z}}_2[\mathcal{E}_\Gamma]$, where, for every $j \in \{1, 2, \dots, r\}$, we have $\alpha_j = 1$, if e_j is connected to b through the arc type a_i , else $\alpha_j = 0$. Now, we are ready to construct the associated process network as we see next.

5.1.4 From a SBGN-PD to a process network (as in Definition 3.1)

Let Γ be a SBGN-PD. Using the notations from 5.1.3, the tuple $(\mathcal{E}_\Gamma, B_\Gamma, \{l_i^\Gamma\}_k)$ forms a process network \mathcal{B}_Γ (as in Definition 3.1) associated to Γ .

Example 5.1. As an illustration for the translation technique discussed above, we will construct the process network associated to the SBGN-PD visualisation of the neuronal/muscle signalling (Figure 23). Let us denote the said SBGN-PD as Γ . We label the process nodes in Γ as b_1, b_2, \dots, b_{12}

without loss of any generality, and thus, according to 5.1.2, $B_\Gamma = \{b_1, b_2, \dots, b_{12}\}$. We now construct the set of entities \mathcal{E}_Γ as prescribed in 5.1.1. In Γ , five compartments are used viz. SYNAPTIC BUTTON, SYNAPTIC VESICULE, SYNAPTIC CLEFT, MUSCLE CYTOSOL AND ER, which we enumerate without loss of generality, as C_1, C_2, C_3, C_4 , and C_5 respectively. For each $i \in \{1, 2, \dots, 5\}$, we define X_i as the set containing ‘meaningful words and symbols’ (w.r.t SBGN-PD, level 1, version 2.0, terminologies [35]) on each entity pool node used and located in the compartment C_i of Γ (as demonstrated in 5.1.1). Let \mathcal{T} denote the set of types of the entity pool nodes used in Γ . Hence, $\mathcal{T} = \{\text{macromolecule, simple chemical, complex}\}$. Let $\mathcal{E}_\Gamma := (\sqcup_{i \in \{1, 2, \dots, 5\}} X_i) \times \mathcal{T}$. For example, the simple chemical ACh in C_1 will be described as $((\text{ACh}, C_1), \text{simple chemical}) \in \mathcal{E}_\Gamma$, whereas, when ACh is in the compartment SYNAPTIC VESICULE, then we represent it as $((\text{ACh}, C_2), \text{simple chemical}) \in \mathcal{E}_\Gamma$, which is distinct from $((\text{ACh}, C_1), \text{simple chemical})$ as an element in \mathcal{E}_Γ . Note that it aligns with the convention in SBGN that identical entity pool nodes located in different compartments are considered different. Let A_Γ denotes the set of connecting arcs used in Γ , and thus $A_\Gamma = \{a_1, a_2, a_3, a_4, a_5\}$, where a_1, a_2, a_3, a_4 and a_5 are consumption arc, catalysis arc, necessary stimulation arc, stimulation arc and production arc, respectively. Now, without loss of any generality, we label the elements of \mathcal{E}_Γ as $e_1, e_2, \dots, e_{23}, e_{24}$ (see Figure 23). Then, for each $i \in \{1, 2, \dots, 5\}$, we define function $l_i^\Gamma: B_\Gamma \rightarrow \bar{\mathbb{Z}}_2[\mathcal{E}_\Gamma]$ that takes $b \in B_\Gamma$ to a formal linear combination $\alpha_1 e_1 + \alpha_2 e_2 + \dots + \alpha_{24} e_{24} \in \bar{\mathbb{Z}}_2[\mathcal{E}_\Gamma]$, where, for every $j \in \{1, 2, \dots, 24\}$, we have $\alpha_j = 1$, if e_j is connected to b through the arc type a_i , else $\alpha_j = 0$. The tuple $(\mathcal{E}_\Gamma, B_\Gamma, \{l_i^\Gamma\}_5)$ forms a process network \mathcal{B}_Γ , which is the process network associated to the SBGN-PD Γ . To illustrate l_i^Γ , let us compute the $l_i^\Gamma(b_1)$ and $l_i^\Gamma(b_{12})$ for all $i = 1, 2, 3, 4, 5$. So, $l_1(b_1) = e_2 + e_1$, $l_2(b_1) = e_3$, $l_3(b_1) = 0$, $l_4(b_1) = 0$ and $l_5(b_1) = e_4$, and for process node b_{12} , we have $l_1(b_{12}) = 0$, $l_2(b_{12}) = 0$, $l_3(b_{12}) = 0$, $l_4(b_{12}) = e_{24}$ and $l_5(b_{12}) = 0$.

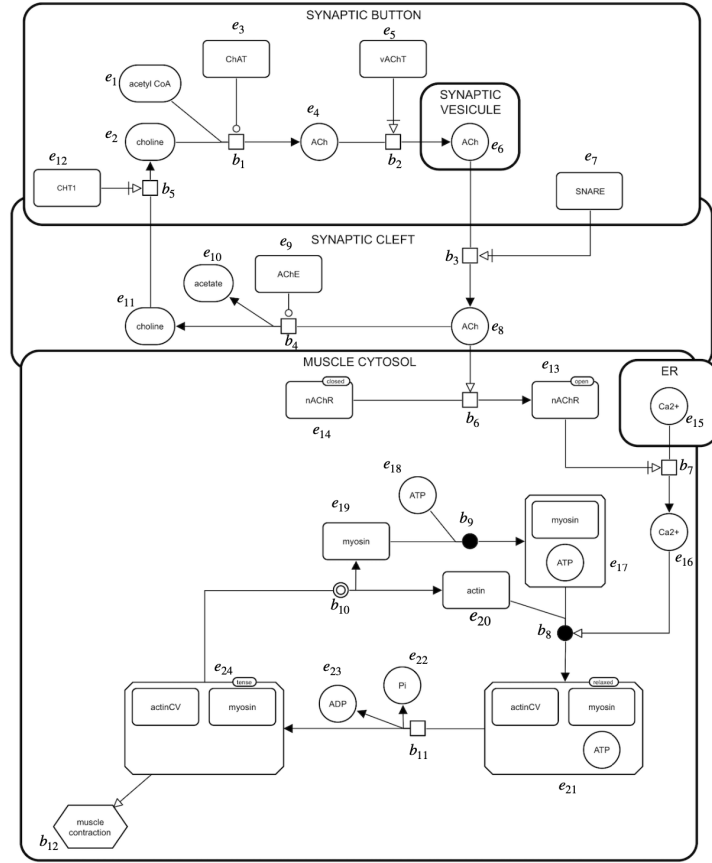


Figure 23: An illustration of the SBGN-PD visualisation of the neuronal/muscle signalling, describing inter-cellular signalling. Here, we labelled the process nodes as $\{b_1, b_2, \dots, b_{12}\}$ and the entity pool nodes as $\{e_1, e_2, \dots, e_{24}\}$. The SBGN image is taken from the neuronal/muscle signalling example on Page 66, [35].

Example 5.2. Let Γ be the SBGN-PD in Figure 1. Since Γ has only one compartment, according to the translation methods discussed above, it is obvious that Example 3.4 gives us the process network associated to Γ .

5.2 SBGN-PD with encapsulation nodes, reference nodes and equivalence arcs

Let Γ be a SBGN-PD with submap(s) (for example consider the IGF signalling (Figure 5), having MAPK cascade as a submap). In the language of process networks, submaps are described as process subnetworks (Definition 4.20) \mathcal{B}'_Γ of \mathcal{B}_Γ , the process network associated to Γ . Interestingly, observe that if Γ is the SBGN PD corresponding to IGF signalling (Figure 5), and \mathcal{B}'_Γ be the subprocess network of \mathcal{B}_Γ , representing the SBGN-PD visualisation of the MAPK cascade, then, if we apply the macroscope $M(\mathcal{B}_\Gamma, \mathcal{B}'_\Gamma)$ (Definition 4.24) of \mathcal{B}'_Γ with respect to \mathcal{B}_Γ , we obtain the reference nodes viz. the macromolecules RAS and ERK associated to the MAPK cascade. This also says that the submap MAPK cascade is connected to the outer network via RAS and ERK. In SBGN, this is expressed by equivalence arcs. More specifically, in the particular case of Figure 5, we have an equivalence arc between RAS and the tag RAS, and an equivalence arc between ERK and the tag ERK.

5.3 SBGN-PD with logical operators and logic arcs

In SBGN-PD, four types of logical operators are used namely *AND operator*, *OR operator*, *NOT operator* and *equivalence operator*, each with a specific purpose. Through examples, we illustrate the translation of SBGN-PD's (with logical operators) to process networks . Consider a portion

of the SBGN-PD visualisation of the activated STAT1 α induction of the IRF1 gene, which uses the AND operator as in Figure 24. Let us denote this SBGN-PD as Γ . Using the methods as discussed above, we construct the set of entities \mathcal{E}_Γ and without loss of any generality, we label its elements as e_1, e_2, e_3 and e_4 , where e_3 denotes an unspecified entity (see Figure 22). The set of process species B_Γ is singleton and contains the element b . Three types of arcs are used here viz. consumption arc, *AND-necessary stimulation arc*, and production arc, which we denote as a_1, a_2 and a_3 . The entities attached to AND-necessary stimulation arc are e_1 and e_2 . Semantically, it means, entities e_1 and e_2 are required for the necessary stimulation for the process b to happen. The corresponding l_1^Γ, l_2^Γ and l_3^Γ are computed according to the method discussed above. Thus, we now have the process network $\mathcal{B}_\Gamma = (\mathcal{E}_\Gamma, B_\Gamma, \{l_i^\Gamma\}_3)$ associated to Γ . Using similar techniques with suitable adaptation, one can convert an SBGN-PD with OR operator, NOT operator and equivalence operator into a process network.

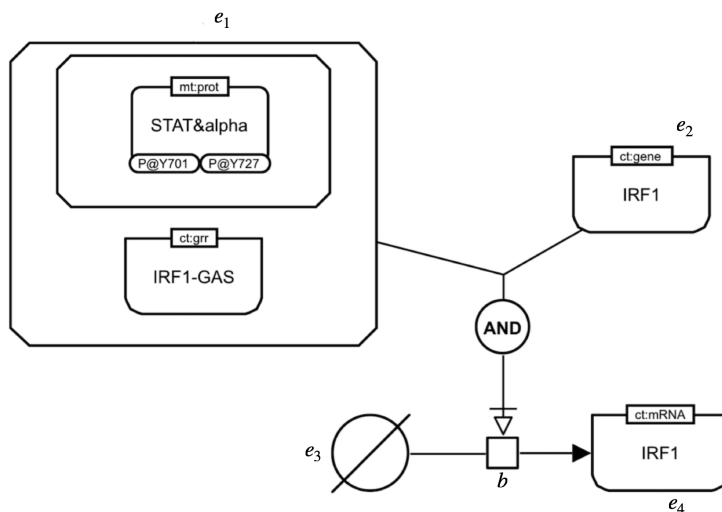


Figure 24: An illustration of gene regulation using AND operator. The SBGN image is derived from the example illustrating the activated STAT1 α induction of the IRF1 gene on Page 67 in [35].

Hence, by appropriately combining the translation methods discussed in this section with the results of Section 3 and Section 4, *one obtains organizational principles* (as stated in Section 1) *for a generic molecular/cellular network visualised in SBGN-PD.*

6 Conclusion and future directions

Our manuscript develops a language rooted in Applied Category Theory for studying organisational principles (as stated in Section 1) for a generic biochemical network admitting a visualisation in Systems Biology Graphical Notation Process Description format. From the nature of the organisational principles studied in this paper, we anticipate that our approach would cast a new light on the *size issue* faced by biologists in studying the behaviour of biochemical reaction networks.

Among many possible future directions, we mention a few here. Besides SBGN-PD, there are two other SBGN languages, viz. SBGN-AF and SBGN-ER. They are also commonly used for visualising biochemical networks at levels of granularity different from the one explored in this paper. It would be interesting to study organisational principles (like the ones studied in this manuscript) for networks visualised in SBGN-AF and SBGN-ER, and investigate the existence of functorial interrelationships between three complimentary SBGN languages viz. SBGN-PD, SBGN-AF and SBGN-ER. Another interesting direction of investigation would be to study the behaviour of SBGN-encoded biochemical networks by the construction an appropriate symmetric monoidal lax double functor whose domain is the symmetric monoidal double category $\text{Open}_{\text{Double}}(\mathbf{Process}_n)$ constructed in Theorem 4.12. We hope that developing a suitable measure of *laxity* (failure of a lax

functor to be a functor) in such a symmetric monoidal lax double functor would bring some new insights into the study of emergent behaviours in the systems of biochemical networks. Finally, for mostly practical reasons, it is important to translate the mathematical techniques developed in this paper to ACT-based computational studies like AlgebraicJulia[41].

7 Acknowledgements

The authors express their gratitude to Heike Siebert for discussions on a preliminary version of this manuscript. They also gratefully acknowledge funding via the Pilot Study 12 – Networked Matter grant of the Life, Light & Matter Interdisciplinary Faculty of the University of Rostock.

References

- [1] Rebekah Aduddell, James Fairbanks, Amit Kumar, Pablo S. Ocal, Evan Patterson, and Brandon T. Shapiro. A compositional account of motifs, mechanisms, and dynamics in biochemical regulatory networks. *Compositionality*, Volume 6 (2024), May 2024. <https://doi.org/10.32408/compositionality-6-2>. URL <https://compositionality.episciences.org/13637>. 2, 3, 16
- [2] Ludovic Roy Alexander Mazein, Andrei Zinovyev. sbgn/cd2sbgnml, August 2023. URL <https://github.com/sbgn/cd2sbgnml>. original-date: 2018-06-27T13:06:22Z, Accessed: (2024-09-30). 2
- [3] Ernst Althaus, Benjamin Merlin Bumpus, James Fairbanks, and Daniel Rosiak. Compositional algorithms on compositional data: Deciding sheaves on presheaves, 2023. URL <https://doi.org/10.48550/arXiv.2302.05575>. 3
- [4] Auckland Bioengineering Institute at the University of Auckland and affiliated research group. The CellML project — CellML, 2021-2024. URL <https://www.cellml.org/>. Accessed: (2024-08-28). 1
- [5] John Baez, Xiaoyan Li, Sophie Libkind, Nathaniel D. Osgood, and Evan Patterson. Compositional modeling with stock and flow diagrams. *Electronic Proceedings in Theoretical Computer Science*, 380:77–96, August 2023. ISSN 2075-2180. <https://doi.org/10.4204/eptcs.380.5>. 3
- [6] John C. Baez and Kenny Courser. Structured cospans, 2020. URL <https://doi.org/10.48550/arXiv.1911.04630>. 2, 3, 16, 17
- [7] John C. Baez and Jade Master. Open Petri nets. *Math. Structures Comput. Sci.*, 30(3): 314–341, 2020. ISSN 0960-1295,1469-8072. <https://doi.org/10.1017/s0960129520000043>. 2, 3, 10, 18, 20
- [8] John C. Baez and Blake S. Pollard. A compositional framework for reaction networks. *Rev. Math. Phys.*, 29(9):1750028, 41, 2017. ISSN 0129-055X,1793-6659. <https://doi.org/10.1142/S0129055X17500283>. 3, 18
- [9] John C. Baez, Kenny Courser, and Christina Vasilakopoulou. Structured versus decorated cospans. *Compositionality*, 4(3):39, 2022. ISSN 2631-4444. <https://doi.org/10.32408/compositionality-4-3>. 2, 3
- [10] Hasan Balci, Metin Can Siper, Nasim Saleh, Ilkin Safarli, Ludovic Roy, Merve Kilicarslan, Rumeysa Ozaydin, Alexander Mazein, Charles Auffray, Özgün Babur, Emek Demir, and Ugur Dogrusoz. Newt: a comprehensive web-based tool for viewing, constructing and analyzing biological maps. *Bioinformatics*, 37(10):1475–1477, June 2021. ISSN 1367-4803, 1367-4811. <https://doi.org/10.1093/bioinformatics/btaa850>. 2
- [11] Frank T. Bergmann, Tobias Czauderna, Ugur Dorusoz, Adrien Rougny, Andreas Dräger, Vasundra Touré, Alexander Mazein, Michael L. Blinov, and Augustin Luna. Systems biology graphical notation markup language (SBGNML) version 0.3. *Journal of Integrative Bioinformatics*, (0):20200016, June 2020. ISSN 1613-4516. <https://doi.org/10.1515/jib-2020-0016>. Place: Berlin, Boston Publisher: De Gruyter. 2
- [12] Kristopher Brown, Evan Patterson, Tyler Hanks, and James Fairbanks. Computational category-theoretic rewriting. *J. Log. Algebr. Methods Program.*, 134:Paper No. 100888, 13, 2023. ISSN 2352-2208,2352-2216. <https://doi.org/10.1016/j.jlamp.2023.100888>. 3

- [13] Safae Cherdal, Salma Mouline, and Souad Amghar. Sbgn2hfpn transformation of sbgn-pd into petri nets illustrated on the glycolysis pathway. *International Journal of Intelligent Engineering & Systems*, 11(5), 2018. URL <https://doi.org/10.22266/ijies2018.1031.26>. 2
- [14] Tobias Czauderna, Christian Klukas, and Falk Schreiber. Editing, validating and translating of SBGN maps. *Bioinformatics*, 26(18):2340–2341, September 2010. ISSN 1367-4803. <https://doi.org/10.1093/bioinformatics/btq407>. 2
- [15] Emek Demir, Michael P. Cary, Suzanne Paley, Ken Fukuda, Christian Lemer, Imre Vastrik, Guanming Wu, Peter D’Eustachio, Carl Schaefer, Joanne Luciano, Frank Schacherer, Irma Martinez-Flores, Zhenjun Hu, Veronica Jimenez-Jacinto, Geeta Joshi-Tope, Kumaran Kandasamy, Alejandra C. Lopez-Fuentes, Huaiyu Mi, Elgar Pichler, Igor Rodchenkov, Andrea Splendiani, Sasha Tkachev, Jeremy Zucker, Gopal Gopinath, Harsha Rajasimha, Ranjani Ramakrishnan, Imran Shah, Mustafa Syed, Nadia Anwar, Özgün Babur, Michael Blinov, Erik Brauner, Dan Corwin, Sylva Donaldson, Frank Gibbons, Robert Goldberg, Peter Hornbeck, Augustin Luna, Peter Murray-Rust, Eric Neumann, Oliver Ruebenacker, Matthias Samwald, Martijn van Iersel, Sarala Wimalaratne, Keith Allen, Burk Braun, Michelle Whirl-Carrillo, Kei-Hoi Cheung, Kam Dahlquist, Andrew Finney, Marc Gillespie, Elizabeth Glass, Li Gong, Robin Haw, Michael Honig, Olivier Hubaut, David Kane, Shiva Krupa, Martina Kutmon, Julie Leonard, Debbie Marks, David Merberg, Victoria Petri, Alex Pico, Dean Ravenscroft, Liya Ren, Nigam Shah, Margot Sunshine, Rebecca Tang, Ryan Whalley, Stan Letovksy, Kenneth H. Buetow, Andrey Rzhetsky, Vincent Schachter, Bruno S. Sobral, Ugur Dogrusoz, Shannon McWeeney, Mirit Aladjem, Ewan Birney, Julio Collado-Vides, Susumu Goto, Michael Hucka, Nicolas Le Novère, Natalia Maltsev, Akhilesh Pandey, Paul Thomas, Edgar Wingender, Peter D. Karp, Chris Sander, and Gary D. Bader. The BioPAX community standard for pathway data sharing. *Nature Biotechnology*, 28(9):935–942, September 2010. ISSN 1546-1696. <https://doi.org/10.1038/nbt.1666>. URL <https://www.nature.com/articles/nbt.1666>. Publisher: Nature Publishing Group. 1
- [16] A. Finney and M. Hucka. Systems biology markup language: Level 2 and beyond. *Biochemical Society Transactions*, 31(Pt 6):1472–1473, December 2003. ISSN 0300-5127. <https://doi.org/10.1042/bst0311472>. 1
- [17] Akira Funahashi, Mineo Morohashi, Hiroaki Kitano, and Naoki Tanimura. Celldesigner: a process diagram editor for gene-regulatory and biochemical networks. *Biosilico*, 1(5):159–162, 2003. [https://doi.org/10.1016/S1478-5382\(03\)02370-9](https://doi.org/10.1016/S1478-5382(03)02370-9). 2
- [18] Akira Funahashi, Yukiko Matsuoka, Akiya Jouraku, Mineo Morohashi, Norihiro Kikuchi, and Hiroaki Kitano. Celldesigner 3.5: A versatile modeling tool for biochemical networks. *Proceedings of the IEEE*, 96(8):1254–1265, August 2008. ISSN 0018-9219. <https://doi.org/10.1109/JPROC.2008.925458>. Funding Information: Manuscript received November 29, 2007; revised January 27, 2008. This work was supported by the ERATO-SORST program (Japan Science and Technology Agency), the International Standard Development area of the International Joint Research Grant (NEDO, Japanese Ministry of Economy, Trade, and Industry), the Strategic Japanese-Swedish Cooperative Program on BMultidisciplinary BIO[(JST-VINNOVA/SSF), the Establishment of a Human Genome Network Platform (MEXT) and through the Japanese Ministry of Education, Culture, Sports, Science, and Technology. A. Funahashi and A. Jouraku are with the Department of Biosciences and Informatics, Keio University, Yokohama 223-8522, Japan (e-mail: funa@bio.keio.ac.jp; jouraku@bio.keio.ac.jp). Y. Matsuoka is with Kitano Symbiotic Systems Project, ERATO-SORST, Tokyo 150-0001, Japan (e-mail: myukiko@symbio.jst.go.jp). M. Morohashi is with PRTM, Tokyo 163-0430, Japan (e-mail: moro@mineo.com). N. Kikuchi is with Mitsui Knowledge Industry Co., Ltd., Tokyo 164-8555, Japan (e-mail: kikuchi-norihiro@mki.co.jp). H. Kitano is with The Systems Biology Institute, Shibuya, Tokyo 150-0001, Japan (e-mail: kitano@sbi.jp). 2
- [19] Piotr Gawron, Marek Ostaszewski, Venkata Satagopam, Stephan Gebel, Alexander Mazein, Michal Kuzma, Simone Zorzan, Fintan McGee, Benoît Otjacques, Rudi Balling, and Reinhard Schneider. MINERVA—a platform for visualization and curation of molecular interaction networks. *npj Systems Biology and Applications*, 2(1):16020, September 2016. ISSN 2056-7189. <https://doi.org/10.1038/npjbsa.2016.20>. 2

- [20] Neil Ghani, Jules Hedges, Viktor Winschel, and Philipp Zahn. Compositional game theory. In *LICS '18—33rd Annual ACM/IEEE Symposium on Logic in Computer Science*, page [10 pp.]. ACM, New York, 2018. ISBN 978-1-4503-5583-4. <https://doi.org/10.1145/3209108.3209165>. 3
- [21] M. Hucka, A. Finney, H. M. Sauro, H. Bolouri, J. C. Doyle, H. Kitano, A. P. Arkin, B. J. Bornstein, D. Bray, A. Cornish-Bowden, A. A. Cuellar, S. Dronov, E. D. Gilles, M. Ginkel, V. Gor, I. I. Goryanin, W. J. Hedley, T. C. Hodgman, J.-H. Hofmeyr, P. J. Hunter, N. S. Juty, J. L. Kasberger, A. Kremling, U. Kummer, N. Le Novère, L. M. Loew, D. Lucio, P. Mendes, E. Minch, E. D. Mjolsness, Y. Nakayama, M. R. Nelson, P. F. Nielsen, T. Sakurada, J. C. Schaff, B. E. Shapiro, T. S. Shimizu, H. D. Spence, J. Stelling, K. Takahashi, M. Tomita, J. Wagner, J. Wang, and and the rest of the SBML Forum:. The systems biology markup language (SBML): a medium for representation and exchange of biochemical network models. *Bioinformatics*, 19(4):524–531, March 2003. ISSN 1367-4803. <https://doi.org/10.1093/bioinformatics/btg015>. 1
- [22] Minoru Kanehisa, Miho Furumichi, Yoko Sato, Yuriko Matsuura, and Mari Ishiguro-Watanabe. KEGG: biological systems database as a model of the real world. *Nucleic Acids Research*, page gkae909, October 1995-2024. ISSN 0305-1048, 1362-4962. <https://doi.org/10.1093/nar/gkae909>. 1
- [23] Sarah M Keating, Dagmar Waltemath, Matthias König, Fengkai Zhang, Andreas Dräger, Claudine Chaouiya, Frank T Bergmann, Andrew Finney, Colin S Gillespie, Tomáš Helikar, Stefan Hoops, Rahuman S Malik-Sheriff, Stuart L Moodie, Ion I Moraru, Chris J Myers, Aurélien Naldi, Brett G Olivier, Sven Sahle, James C Schaff, Lucian P Smith, Maciej J Swat, Denis Thieffry, Leandro Watanabe, Darren J Wilkinson, Michael L Blinov, Kimberly Begley, James R Faeder, Harold F Gómez, Thomas M Hamm, Yuichiro Inagaki, Wolfram Liebermeister, Allyson L Lister, Daniel Lucio, Eric Mjolsness, Carole J Proctor, Karthik Raman, Nicolas Rodriguez, Clifford A Shaffer, Bruce E Shapiro, Joerg Stelling, Neil Swainston, Naoki Tanimura, John Wagner, Martin Meier-Schellersheim, Herbert M Sauro, Bernhard Palsson, Hamid Bolouri, Hiroaki Kitano, Akira Funahashi, Henning Hermjakob, John C Doyle, Michael Hucka, SBML Level 3 Community members, Richard R Adams, Nicholas A Allen, Bastian R Angermann, Marco Antonioti, Gary D Bader, Jan Červený, Mélanie Courtot, Chris D Cox, Piero Dalle Pezze, Emek Demir, William S Denney, Harish Dharuri, Julien Drier, Dirk Drasdo, Ali Ebrahim, Johannes Eichner, Johan Elf, Lukas Ender, Chris T Evelo, Christoph Flamm, Roman MT Fleming, Martina Fröhlich, Mihai Glont, Emanuel Gonçalves, Martin Golebiewski, Hovakim Grabski, Alex Gutteridge, Damon Hachmeister, Leonard A Harris, Benjamin D Heavner, Ron Henkel, William S Hlavacek, Bin Hu, Daniel R Hyduke, Hidde de Jong, Nick Juty, Peter D Karp, Jonathan R Karr, Douglas B Kell, Roland Keller, Ilya Kiselev, Steffen Klamt, Edda Klipp, Christian Knüpfer, Fedor Kolpakov, Falko Krause, Martina Kutmon, Camille Laibe, Conor Lawless, Lu Li, Leslie M Loew, Rainer Machne, Yukiko Matsuoka, Pedro Mendes, Huaiyu Mi, Florian Mittag, Pedro T Monteiro, Kedar Nath Natarajan, Poul MF Nielsen, Tramy Nguyen, Alida Palmisano, Jean-Baptiste Pettit, Thomas Pfau, Robert D Phair, Tomas Radivoyevitch, Johann M Rohwer, Oliver A Ruebenacker, Julio Saez-Rodriguez, Martin Scharm, Henning Schmidt, Falk Schreiber, Michael Schubert, Roman Schulte, Stuart C Sealfon, Kieran Smallbone, Sylvain Soliman, Melanie I Stefan, Devin P Sullivan, Koichi Takahashi, Bas Teusink, David Tolnay, Ibrahim Vazirabad, Axel von Kamp, Ulrike Wittig, Clemens Wrzodek, Finja Wrzodek, Ioannis Xenarios, Anna Zhukova, and Jeremy Zucker. SBML Level 3: an extensible format for the exchange and reuse of biological models. *Molecular Systems Biology*, 16(8):e9110, August 2020. ISSN 1744-4292. <https://doi.org/10.15252/msb.20199110>. URL <https://www.embopress.org/doi/full/10.15252/msb.20199110>. Publisher: John Wiley & Sons, Ltd. 1
- [24] Kanehisa Laboratories. KGML (KEGG Markup Language), 1995-2024. URL <https://www.kegg.jp/kegg/xml/>. Accessed: (2024-08-27). 1
- [25] Nicolas Le Novère, Michael Hucka, Huaiyu Mi, Stuart Moodie, Falk Schreiber, Anatoly Sorokin, Emek Demir, Katja Wegner, Mirit I. Aladjem, Sarala M. Wimalaratne, Frank T. Bergman, Ralph Gauges, Peter Ghazal, Hideya Kawaji, Lu Li, Yukiko Matsuoka, Alice Viléger, Sarah E. Boyd, Laurence Calzone, Melanie Courtot, Ugur Dogrusoz, Tom C. Freeman, Akira Funahashi, Samik Ghosh, Akiya Jouraku, Sohyoung Kim, Fedor Kolpakov, Augustin

- Luna, Sven Sahle, Esther Schmidt, Steven Watterson, Guanming Wu, Igor Goryanin, Douglas B. Kell, Chris Sander, Herbert Sauro, Jacky L. Snoep, Kurt Kohn, and Hiroaki Kitano. The Systems Biology Graphical Notation. *Nature Biotechnology*, 27(8):735–741, August 2009. ISSN 1546-1696. <https://doi.org/10.1038/nbt.1558>. 2
- [26] Sophie Libkind, Andrew Baas, Micah Halter, Evan Patterson, and James P. Fairbanks. An algebraic framework for structured epidemic modelling. *Philos. Trans. Roy. Soc. A*, 380(2233):Paper No. 20210309, 17, 2022. ISSN 1364-503X,1471-2962. <https://doi.org/10.1098/rsta.2021.0309>. 3
- [27] Sophie Libkind, Andrew Baas, Evan Patterson, and James Fairbanks. Operadic modeling of dynamical systems: Mathematics and computation. *Electronic Proceedings in Theoretical Computer Science*, 372:192–206, November 2022. ISSN 2075-2180. <https://doi.org/10.4204/eptcs.372.14>. 3
- [28] Laurence Loewe, Maria Luisa Guerriero, Steven Watterson, Stuart Moodie, Peter Ghazal, and Jane Hillston. *Translation from the Quantified Implicit Process Flow Abstraction in SBGN-PD Diagrams to Bio-PEPA Illustrated on the Cholesterol Pathway*, pages 13–38. Springer Berlin Heidelberg, Berlin, Heidelberg, 2011. ISBN 978-3-642-19748-2. https://doi.org/10.1007/978-3-642-19748-2_2. 2
- [29] Rahuman S Malik-Sheriff, Mihai Glont, Tung V N Nguyen, Krishna Tiwari, Matthew G Roberts, Ashley Xavier, Manh T Vu, Jinghao Men, Matthieu Maire, Sarubini Kananathan, Emma L Fairbanks, Johannes P Meyer, Chinmay Arankalle, Thawfeek M Varusai, Vincent Knight-Schrijver, Lu Li, Corina Dueñas-Roca, Gaurhari Dass, Sarah M Keating, Young M Park, Nicola Buso, Nicolas Rodriguez, Michael Hucka, and Henning Hermjakob. BioModels—15 years of sharing computational models in life science. *Nucleic Acids Research*, 48(D1):D407–D415, November 2019. ISSN 0305-1048. <https://doi.org/10.1093/nar/gkz1055>. [_eprint: https://academic.oup.com/nar/article-pdf/48/D1/D407/31698010/gkz1055.pdf](https://academic.oup.com/nar/article-pdf/48/D1/D407/31698010/gkz1055.pdf). 2
- [30] Jade Master. Composing behaviors of networks, 2021. URL <https://doi.org/10.48550/arXiv.2105.12905>. 3
- [31] Huaiyu Mi, Falk Schreiber, Stuart Moodie, Tobias Czauderna, Emek Demir, Robin Haw, Augustin Luna, Nicolas Le Novère, Anatoly Sorokin, and Alice Villéger. Systems Biology Graphical Notation: Activity Flow language Level 1 Version 1.2. *Journal of Integrative Bioinformatics*, 12(2):265, September 2015. ISSN 1613-4516. <https://doi.org/10.2390/biecoll-jib-2015-265>. 2
- [32] Evan Patterson, Owen Lynch, and James Fairbanks. Categorical data structures for technical computing. *Compositionality*, 4(5):27, 2022. ISSN 2631-4444. <https://doi.org/10.32408/compositionality-4-5>. 3
- [33] Blake S. Pollard. A second law for open Markov processes. *Open Syst. Inf. Dyn.*, 23(1):1650006, 11, 2016. ISSN 1230-1612,1793-7191. <https://doi.org/10.1142/S1230161216500062>. 3, 18
- [34] Adrien Rougny, Christine Froidevaux, Laurence Calzone, and Loïc Paulevé. Qualitative dynamics semantics for sbgn process description. *BMC systems biology*, 10:1–24, 2016. URL <https://doi.org/10.1186/s12918-016-0285-0>. 2
- [35] Adrien Rougny, Vasundra Touré, Stuart Moodie, Irina Balaur, Tobias Czauderna, Hanna Borlinghaus, Ugur Dogrusoz, Alexander Mazein, Andreas Dräger, Michael L. Blinov, Alice Villéger, Robin Haw, Emek Demir, Huaiyu Mi, Anatoly Sorokin, Falk Schreiber, and Augustin Luna. Systems Biology Graphical Notation: Process Description language Level 1 Version 2.0. *Journal of Integrative Bioinformatics*, 16(2), June 2019. ISSN 1613-4516. <https://doi.org/10.1515/jib-2019-0022>. 2, 5, 6, 7, 8, 11, 26, 29, 30, 32, 33, 34
- [36] David E. Rydeheard and Rod M. Burstall. *Computational category theory*. Prentice Hall International Series in Computer Science. Prentice Hall International, Englewood Cliffs, NJ, 1988. ISBN 0-13-162736-8. URL <https://doi.org/10.1017/CB09780511608872.008>. With a foreword by John W. Gray. 16
- [37] Mecit Sari, Istemi Bahceci, Ugur Dogrusoz, Selcuk Onur Sumer, Bülent Arman Aksoy, Özgün Babur, and Emek Demir. SBGNViz: A Tool for Visualization and Complexity Management of SBGN Process Description Maps. *PLOS ONE*, 10(6):e0128985, June 2015. ISSN 1932-6203. <https://doi.org/10.1371/journal.pone.0128985>. 2

- [38] Charles N. Serhan, Shailendra K. Gupta, Mauro Perretti, Catherine Godson, Eoin Brennan, Yongsheng Li, Oliver Soehnlein, Takao Shimizu, Oliver Werz, Valerio Chiurchiù, Angelo Azzi, Marc Dubourdeau, Suchi Smita Gupta, Patrick Schopohl, Matti Hoch, Dragana Gjorgevikj, Faiz M. Khan, David Brauer, Anurag Tripathi, Konstantin Cesnulevicius, David Lescheid, Myron Schultz, Eva Särndahl, Dirk Repsilber, Robert Kruse, Angelo Sala, Jesper Z. Haeggström, Bruce D. Levy, János G. Filep, and Olaf Wolkenhauer. The atlas of inflammation resolution (air). *Molecular Aspects of Medicine*, 74:100894, 2020. ISSN 0098-2997. <https://doi.org/10.1016/j.mam.2020.100894>. URL <https://www.sciencedirect.com/science/article/pii/S0098299720300960>. The Atlas of Inflammation Resolution (AIR). 2
- [39] Anatoly Sorokin, Nicolas Le Novère, Augustin Luna, Tobias Czauderna, Emek Demir, Robin Haw, Huaiyu Mi, Stuart Moodie, Falk Schreiber, and Alice Villéger. Systems Biology Graphical Notation: Entity Relationship language Level 1 Version 2. *Journal of Integrative Bioinformatics*, 12(2):264, September 2015. ISSN 1613-4516. <https://doi.org/10.2390/biecoll-jib-2015-264>. 2
- [40] MJ Swat, S Moodie, SM Wimalaratne, NR Kristensen, M Lavielle, A Mari, P Magni, MK Smith, R Bizzotto, L Pasotti, E Mezzalana, E Comets, C Sarr, N Terranova, E Blaudez, P Chan, J Chard, K Chatel, M Chenel, D Edwards, C Franklin, T Giorgino, M Glont, P Girard, P Grenon, K Harling, AC Hooker, R Kaye, R Keizer, C Kloft, JN Kok, N Kokash, C Laibe, C Laveille, G Lestini, F Mentré, A Munafo, R Nordgren, HB Nyberg, ZP Parra-Guillen, E Plan, B Ribba, G Smith, IF Trocóniz, F Yvon, PA Milligan, L Harnisch, M Karlsson, H Hermjakob, and N Le Novère. Pharmacometrics markup language (pharmml): Opening new perspectives for model exchange in drug development. *CPT: Pharmacometrics & Systems Pharmacology*, 4(6):316–319, 2015. <https://doi.org/10.1002/psp4.57>. URL <https://ascpt.onlinelibrary.wiley.com/doi/abs/10.1002/psp4.57>. 1
- [41] The AlgebraicJulia team. AlgebraicJulia. URL <https://www.algebraicjulia.org/>. Accessed: (2024-10-21). 3, 35
- [42] Vasundra Touré, Alexander Mazein, Dagmar Waltemath, Irina Balaur, Mansoor Saqi, Ron Henkel, Johann Pellet, and Charles Auffray. STON: exploring biological pathways using the SBGN standard and graph databases. *BMC Bioinformatics*, 17(1):494, December 2016. ISSN 1471-2105. <https://doi.org/10.1186/s12859-016-1394-x>. 2
- [43] Roland Wiese. wiese42/krayon4sbgn, April 2024. URL <https://github.com/wiese42/krayon4sbgn>. original-date: 2018-08-21T09:08:42Z, Accessed: (2024-09-30). 2